Supplementary Information for : Investigation of the intermolecular origins of high and low heats of fusion in azolium salt phase change materials for thermal energy storage

Saliha Saher,[a] Samantha L . Piper,[a] Craig M. Forsyth,[a] Mega Kar,[b] Douglas R. MacFarlane, [a] Jennifer M. Pringle,[b] Karolina Matuszek,[a]

[a]School of Chemistry, Monash University, Clayton, VIC 3800, Australia

[b]Institute of Frontier Materials, Deakin University, 221 Burwood, VIC 3125, Australia.

email: douglas.macfarlane@monash.edu, Karolina.matuszek@monash.edu,

Table of Contents

1. Supplementary Discussion 2
1.1. **Chloride salts** 2
1.2 Ethane sulfonates 3
2. Materials 5
3. Spectroscopic Analysis 5
3.1 Imidazolium salts 5
3.2 1,2,4-triazolium salts 6
3.3. NMR plots of imidazolium and 1,2,4-triazolium salts 6
4.0 Single Crystal X-ray crystallography 15
4.1 Chlorides 18
4.2 Mesylates 19
4.3 Ethanesulfonate 20
4.4 Triflate 22
4.5 Benzensulfonate 23
4.6 Hydrogen sulfate 25
5 Hirshfeld surface analysis 27
6 Differential Scanning Calorimetry (DSC) plots 33
7 Thermogravimetric analysis 34

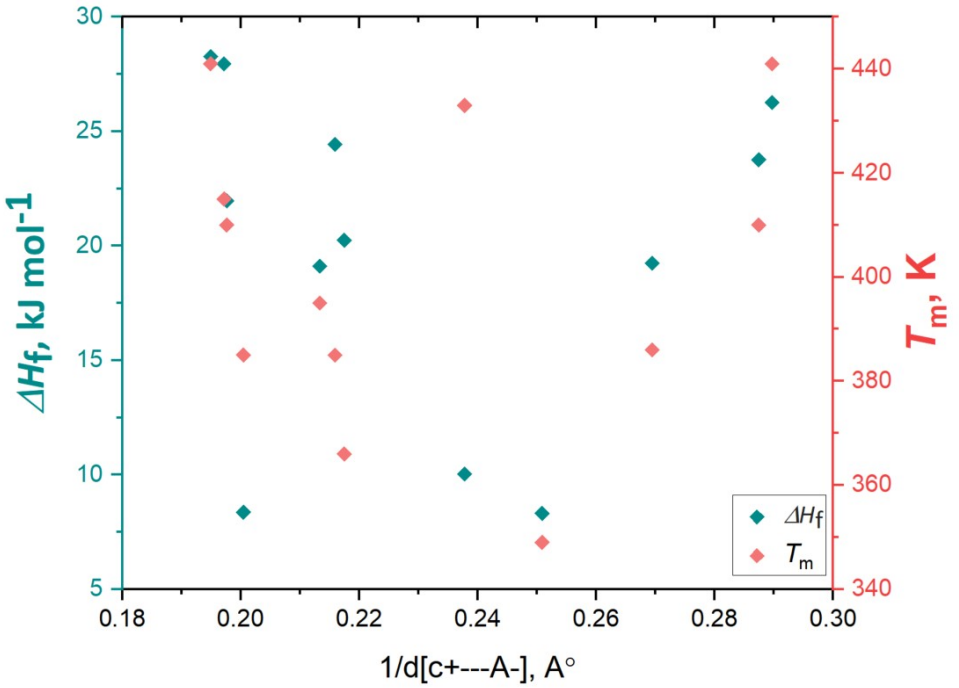

Figure S 1 The correlation between coulombic interactions melting enthalpy and melting point in azolium salts (excluding salts with solid-solid transition).

1. Supplementary Discussion

1.1. Chloride salts

The chloride anion has weak H-bond forming ability, which is reflected in the long H-bond distances (all are > 3.000 Å) in the three chloride salts compared to all other tested anions. The longer and weaker H-bonds justify the lowest enthalpy of fusion of imidazolium chloride, pyrazolium chloride and triazolium chloride in their respective cation series.

The asymmetric unit of these three chloride salts have different numbers of ion pairs: [Im]Cl has eight ion pairs, [Tri]Cl has two ion pairs and [Pzy]Cl has one ion pair in the asymmetric

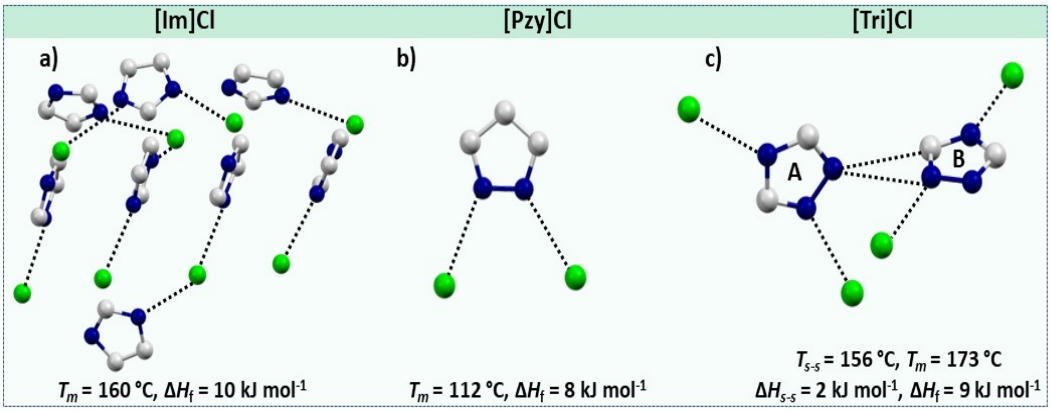

unit, therefore, instead of individual H-bond lengths and angles, average H-bond lengths and

Figure S2 H-bonding in a) eight ion pairs in asymmetric unit of [Im]Cl, b) [Pzy]Cl and c) two ion pairs in asymmetric unit of [Tri]Cl.

angles are discussed here. [Tri]Cl has the highest total enthalpy (ΔH_f = 11 kJ mol^{-1}) among the three chloride salts (including the enthalpy of solid-solid transition $\Delta H_{s\text{-}s}$ = 2 kJ mol^{-1}). It has two cations in the asymmetric unit, with a three-dimensional network of H-bonds (shown as ring A and B in Figure S1). One cation participates in H-bonding with two chloride ions [avg. d(N···Cl = 3.0645 Å), avg. ∠(N-H···Cl) = 173.15 °] and the other cation makes only one H-bond with the chloride anion [d(N···Cl = 3.079 Å), ∠(N-H···Cl) = 172.63 °]. Another potential interaction is the N-H···N bond between adjacent triazolium rings, which is comparable in length [d(N···N = 3.072 Å) with the N-H···Cl bond but has poor linearity [∠(N-H···N) = 116.61 °]. This non-linear weak ring-ring interaction may break down quite easily, resulting in reorientation of rings, which might be one of the origins of the observed solid-solid phase transitions.

[Pzy]Cl has two H-bonds per cation [avg. d(N···Cl = 3.037Å), avg. ∠(N-H···Cl) = 157.93 °] which are slightly shorter but less linear and hence weaker than those of [Tri]Cl, accounting for the lower melting enthalpy (ΔH_f = 8 kJ mol^{-1}). [Im]Cl, however, has a unique crystal structure with eight ion pairs in the asymmetric unit. The large number of ion pairs in the asymmetric unit are presumably the result of conflict between the N-H···Cl interactions and close packing of the imidazolium chloride ions. Similar conflict between linear O-H···H interactions and the steric demand of substituents in alcohols result in frustration in crystal packing and more than one molecule in the asymmetric unit.[1,2] The cut-off distance for measuring H-bonding was kept at 3.2 Å for this salt, particularly as the arrangement of ions is unique in imidazolium chloride and all H-bonds contribute to stabilization of the observed crystal structure. The H-bond (avg. d(N···Cl = 3.094 Å),avg. ∠(N-H···Cl) = 164.6 °) in [Im]Cl is slightly longer than in pyrazolium and triazolium but it is slightly more linear. It should be mentioned that [Im]Cl undergo two solid-solid phase transitions (phase I, $T_{s\text{-}s}$ = -9 °C, Δ $H_{s\text{-}s}$ = 0.6 kJ mol^{-1} and phase II $T_{s\text{-}s}$= -96 °C, $\Delta H_{s\text{-}s}$ = 0.2 kJ mol^{-1}) but these transitions were not reproducible in repeated DSC.

All three salts have Hirshfeld plots (Figure S 52) with two H···Cl interaction spikes constituting 39 %, 42 % and 41 % of total interactions in [Im]Cl, [Pzy]Cl and [Tri]Cl, respectively. The inner pair of broad peaks in [Tri]Cl adjacent to the outer spikes show significantly higher N···H interactions (24%) than in [Im]Cl (8 %, scattered points) and [Pzy]Cl (9 % spread and less sharp). This is consistent with [Tri]Cl having slightly higher ΔH_f. The central broad peak

corresponds to H···H interactions that contribute 33 % in [Im]Cl, 32 % in [Pzy]Cl and 19 % in [Tri]Cl.

1.2 Ethane sulfonates

We further investigated the ethanesulfonate salts and anticipated that the slightly enhanced electron-donating effect of the ethyl chain should lead to increased availability of electron density on the oxygen atoms of the sulfonate anion. Figure S2 shows that the H-bonding pattern in all three salts differ markedly, but the melting enthalpies are relatively similar. The

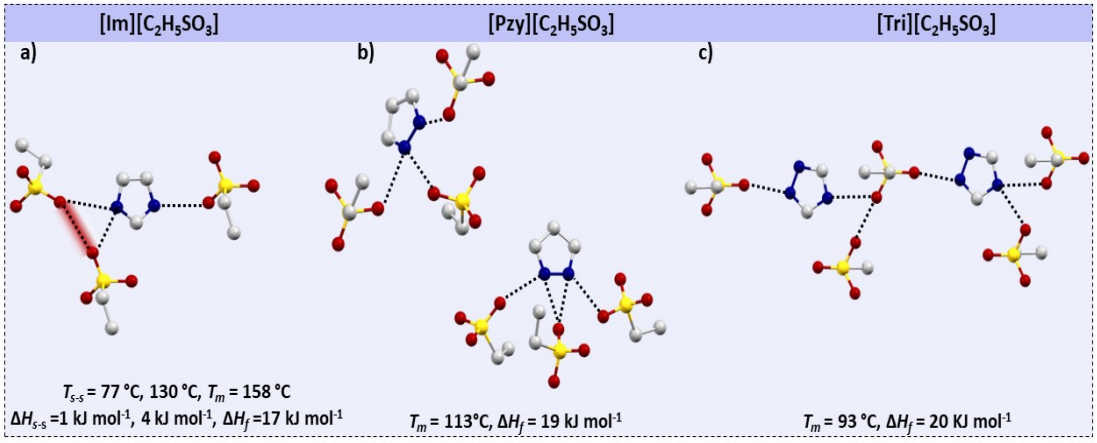

Figure S3 H-bonding pattern in the single crystal structure of a) [Im][$C_2H_5SO_3$], b) [Pzy][$C_2H_5SO_3$] and c) [Tri][$C_2H_5SO_3$]. The [Pzy][$C_2H_5SO_3$] and [Tri][$C_2H_5SO_3$] has two ion pairs in asymmetric unit and each of two cations establish different H-bonding pattern. For simplicity, hydrogen atoms are not displayed.

enhanced H-bond acceptor ability seems to result in higher bifurcation of H-bonds which makes it difficult to compare the strength of H-bonds. [Pzy][$C_2H_5SO_3$] and [Tri][$C_2H_5SO_3$] contain two ion pairs in the asymmetric unit (ASU) and each ion pair has a unique H-bonding pattern. [Tri][$C_2H_5SO_3$], having the lowest melting point and highest enthalpy (T_m = 93 °C, ΔH_f = 20 kJ mol^{-1}) among the three salts, has one cation participating in two canonical H-bonds [d(N···O) = 2.661 Å ∠(N-H···O) = 151.17 ° & d(N···O) = 2.761Å ∠(N-H···O) = 146.83°] and the other cation (Figure 5c) has one canonical (d(N···O) = 2.660 Å, ∠(N-H···O) = 153.34°) and two bifurcated H-bonds [d(N···O) = 2.998 Å ∠(N-H···O) = 125.38 ° & d(N···O) = 2.769 Å ∠(N-H···O) = 146.07 °].

[Pzy][$C_2H_5SO_3$] melts at 113°C with slightly lower enthalpy (ΔH_f = 19 kJ mol^{-1}) than the triazolium analogue. One cation in [Pzy][$C_2H_5SO_3$] interacts with three neighbouring anions by three H-bonds (avg. d(N···O) = 2.745 Å, avg. ∠(N-H···O) = 144.51 °) while the other cation (Figure 5b) forms four bifurcated H-bonds (avg. d(N···O) = 2.790 Å, avg. ∠(N-H···O) = 131.88 °). The cations and anions are not in one plane, they build a 3D H-bonding network.

[Im][$C_2H_5SO_3$] has two solid-solid transitions, at 77 °C and 130 °C, with enthalpies of 1 and 4 kJ mol^{-1} respectively, before melting at 158 °C (ΔH_f = 17kJ mol^{-1}). This salt has one ion pair in the asymmetric unit and the cation is surrounded by three anions, one linked through a canonical H-bond and to the other two anions by bifurcated H-bonds, as shown in Figure 5. The average H-bond length d(N···O) = 2.928 Å, avg. ∠(N-H···O) = 141.88 °) is longer than in the other two salts.

The Hirshfeld surface of [Pzy][$C_2H_5SO_3$] and [Tri][$C_2H_5SO_3$] is generated for one ion pair only (Figure S55), The Hirshfeld surface of [Im][$C_2H_5SO_3$] has sharp spikes corresponding to O···H interactions and has a slightly higher proportion of O···H interactions (40 %) compared to 39 % in [Pzy][$C_2H_5SO_3$] and 37 % in [Tri][$C_2H_5SO_3$]. Interestingly, the major interactions are H···H interactions appearing as a broad central peak, making 43 % and 43 % of all interactions in [Im][$C_2H_5SO_3$] and [Pzy][$C_2H_5SO_3$] respectively. The percentage of O···H and H···H interactions in [Tri][$C_2H_5SO_3$] is nearly same (36%).

2. Materials

The chemicals imidazole (Merck), 1,2,4-triazole (Alfa Aesar), methane sulfonic acid (Sigma Alrich), ethane sulfonic acid (Sigma-Aldrich), trifluoroethane sulfonic acid (Sigma-Aldrich) Scientific), benzenesulfonic acid (Sigma Aldrich), sulfuric acid, hydrochloric acid, and solvents were used without further purification.

3. Spectroscopic Analysis

Nuclear Magnetic Resonance Spectroscopy (NMR):

NMR spectroscopy was performed using a Bruker Avance III 400 (400.13 MHz, 1 H; 100.6 MHz, 13 C) with a BBFO probe. All spectra were acquired at 298 K unless otherwise stated. NMR spectra were processed using the Bruker TOPSPIN 4.1 software. Chemical shifts (δ) are reported in ppm and were referenced to the residual solvent signals.

3.1 Imidazolium salts

[Im]Cl

^{1}H NMR (400 MHz, d_6-DMSO) δ 9.10 (1H), 7.66 (2H). **^{13}C NMR** (100.1 MHz, d_6-DMSO) δ 134.41, 119.69.

[Im][HSO_4]

^{1}H NMR (400 MHz, d_6-DMSO) δ 11.53 (2H), 9.02 (1H), 7.64 (2H). **^{13}C NMR** (100.1 MHz, d_6-DMSO) δ 134.84, 119.86.

[Im][CH_3SO_3]

^{1}H NMR (400 MHz, d_6-DMSO) δ 14.33 (1H), 9.09 (1H), 7.69 (2H) δ 2.38 **^{13}C NMR** (100.1 MHz, d_6-DMSO) δ. 134.82, 119.78, 39.84.

[Im][$C_2H_5SO_3$]

^{1}H NMR (400 MHz, d_6-DMSO) δ 9.07 (1H), 7.69 (2H), 2.39 (quartet, 2H), δ 1.07 (triplet, 2H). **^{13}C NMR** (100.1 MHz, d_6-DMSO) δ. 134.83, 119.80, 45.68, 10.24.

[Im][CF_3SO_3]

^{1}H NMR (400 MHz, d_6-DMSO) δ 9.07 (1H), 7.69 (2H) **^{13}C NMR** (100.1 MHz, d_6-DMSO) δ 134.75, 122.68, 119.73.

[Im][$C_6H_5SO_3$]

^{1}H NMR (400 MHz, d_6-DMSO) δ 9.09 (1H), 7.69 (doublet, 2H), δ 7.61 (quartet, 2H), 7.32 (multiplet, 3H) **^{13}C NMR** (100.1 MHz, d_6-DMSO) δ 147.93, 134.84, 129.38, 128.35, 125.80, 119.80.

3.2 1,2,4-triazolium salts

Nuclear Magnetic Resonance Spectroscopy (NMR):

[Tri]Cl

^{1}H NMR (400 MHz, d_6-DMSO) δ 8.9 (2H) **^{13}C NMR** (100.1 MHz, d_6-DMSO) δ 143.12.

[Tri][HSO_4]

^{1}H NMR (400 MHz, d_6-DMSO) δ12.80 (2H), 9.26 (1H) **^{13}C NMR** (100.1 MHz, d_6-DMSO) δ 143.42.

[Tri][CH_3SO_3]

^{1}H NMR (400 MHz, d_6-DMSO) δ 8.9 (2H), 2.3 (3H) **^{13}C NMR** (100.1 MHz, d_6-DMSO) δ 143.74, 40.3.

[Tri][$C_2H_5SO_3$]

^{1}H NMR (400 MHz, d_6-DMSO) δ 9.10 (2H), 2.08 (2H), 1.09 (3H) **^{13}C NMR** (100.1 MHz, d_6-DMSO) δ 143.45, 45.70, 10.02.

[Tri][CF_3SO_3]

^{1}H NMR (400 MHz, d_6-DMSO) δ 14.60 (2H), 9.36 (2H) **^{13}C NMR** (100.1 MHz, d_6-DMSO) δ. 143.34, 125.89, 122.69, 119.49, 116.29.

[Tri][$C_6H_5SO_3$]

^{1}H NMR (400 MHz, d_6-DMSO) δ 8.91 (2H), 7.59 (doublet of doublet, 2H), 7.31 (m, 3H) **^{13}C NMR** (100.1 MHz, d_6-DMSO) δ. 147.80, 14335, 128.35, 125.93.

3.3. NMR plots of imidazolium and 1,2,4-triazolium salts

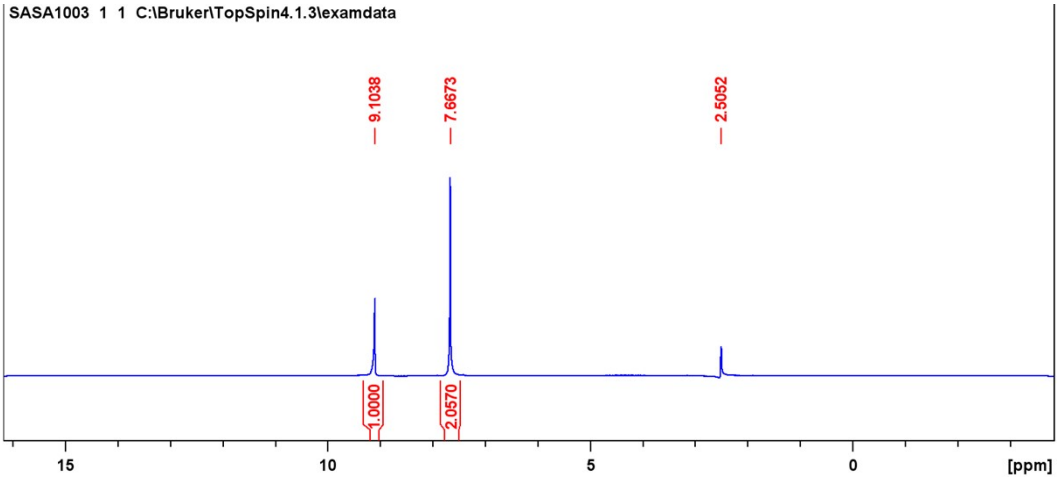

Figure S4 ^{1}HNMR [Im] Cl.

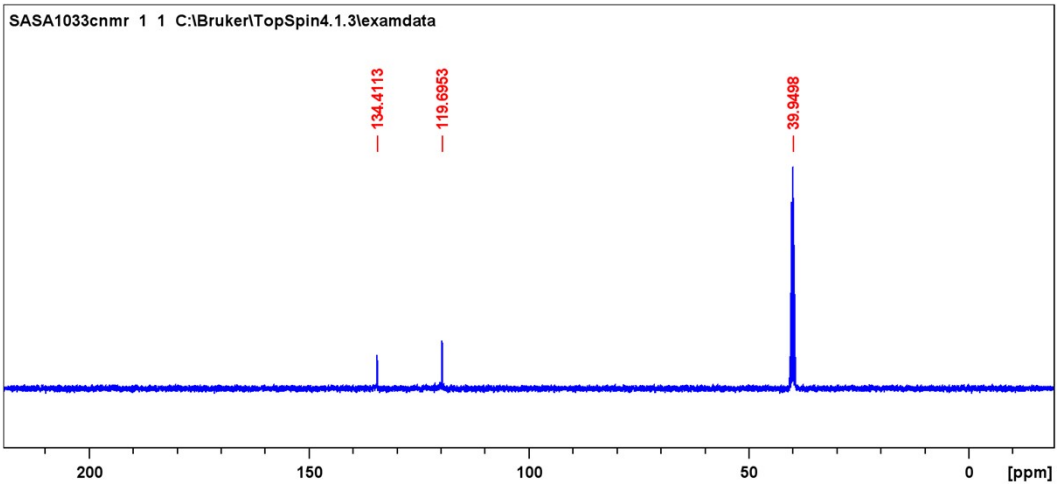

Figure S5 ^{13}CNMR [Im]Cl.

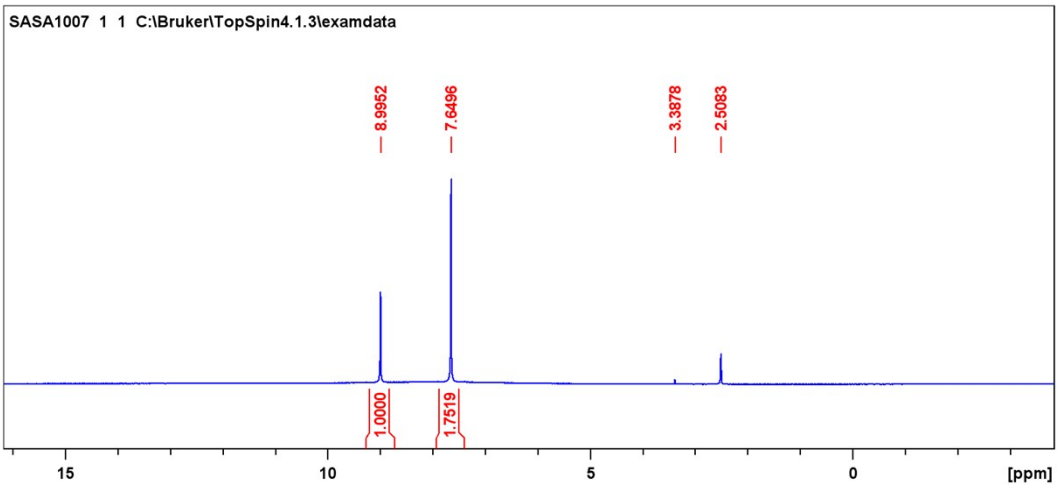

Figure S6 [1]HNMR of [Im][HSO_4].

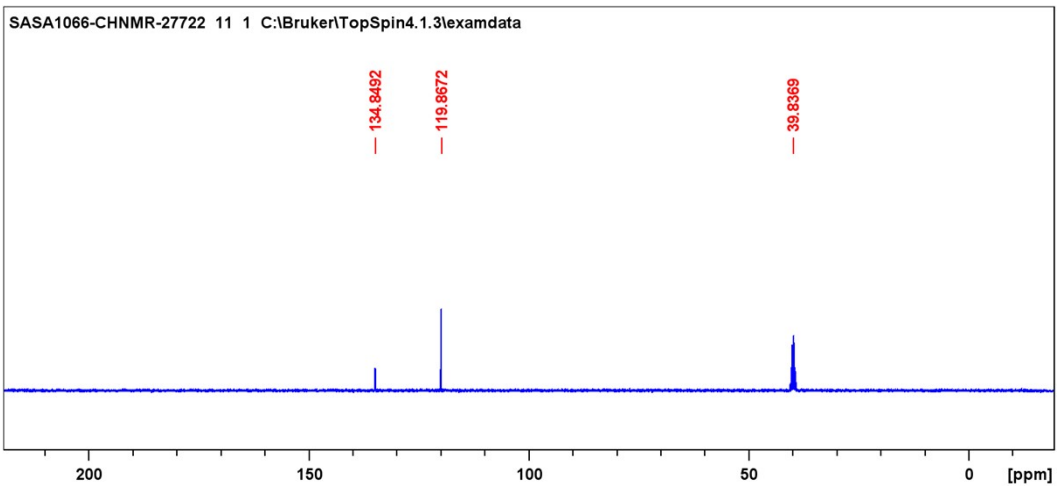

Figure S7 [13]CNMR of [Im][HSO_4].

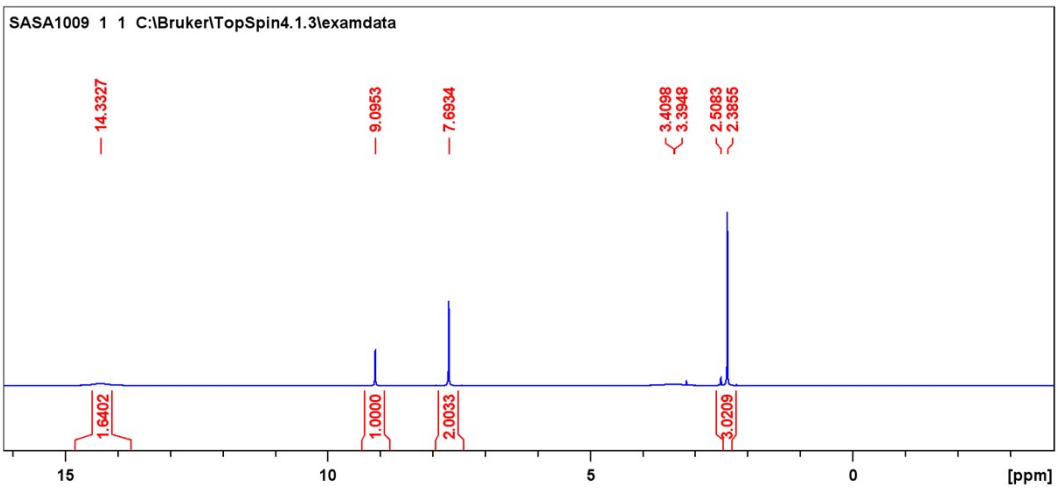

Figure S8 [1]HNMR of [Im][CH_3SO_3].

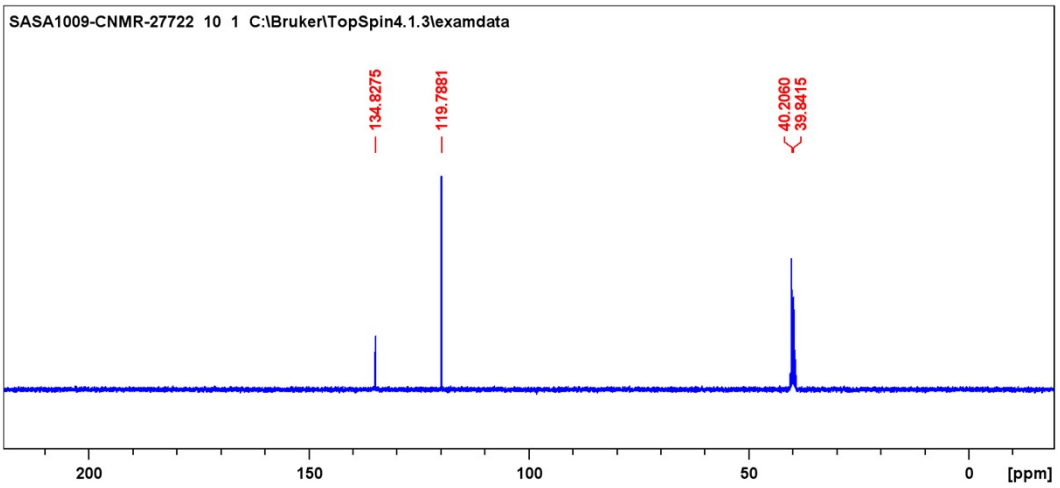

Figure S9 ^{13}CNMR of [Im][CH_3SO_3].

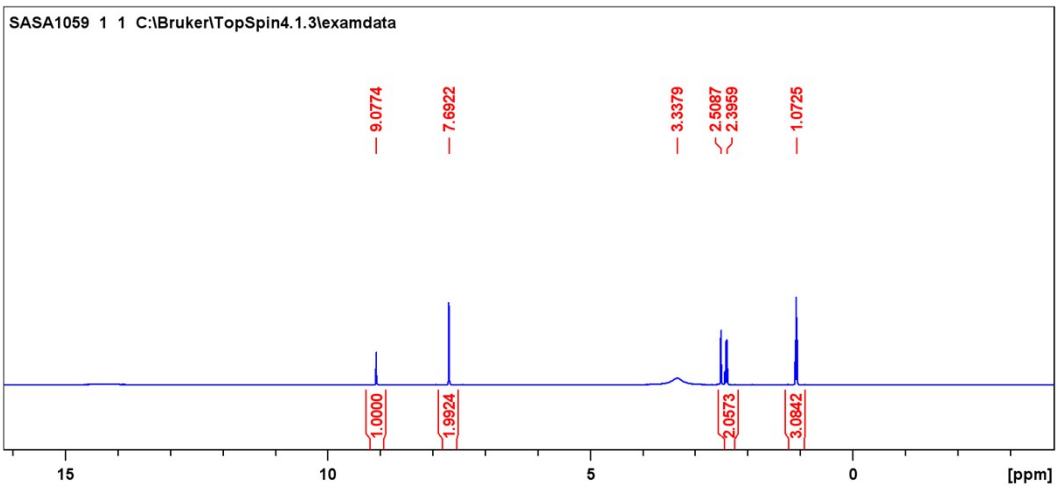

Figure S10 ^{1}HNMR of [Im][$C_2H_5SO_3$].

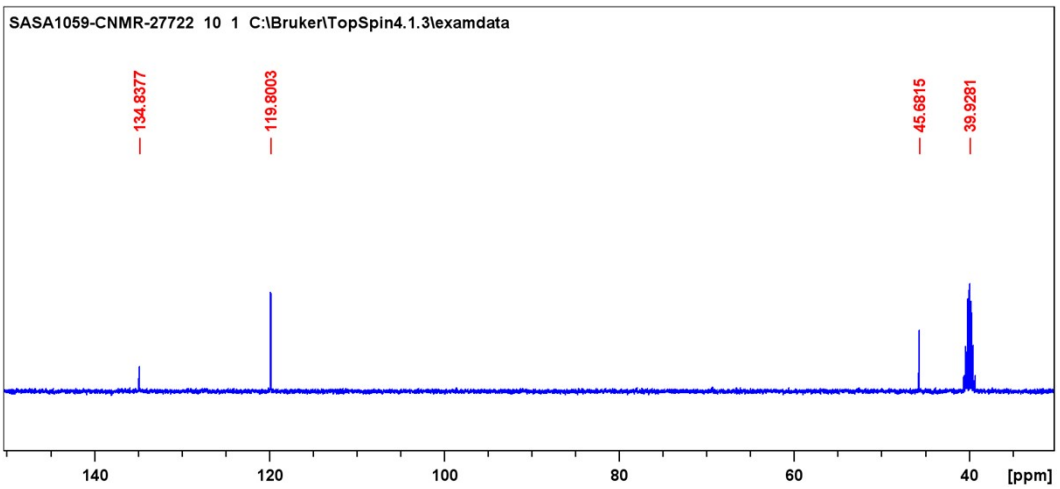

Figure S11 ^{13}CNMR of [Im][$C_2H_5SO_3$].

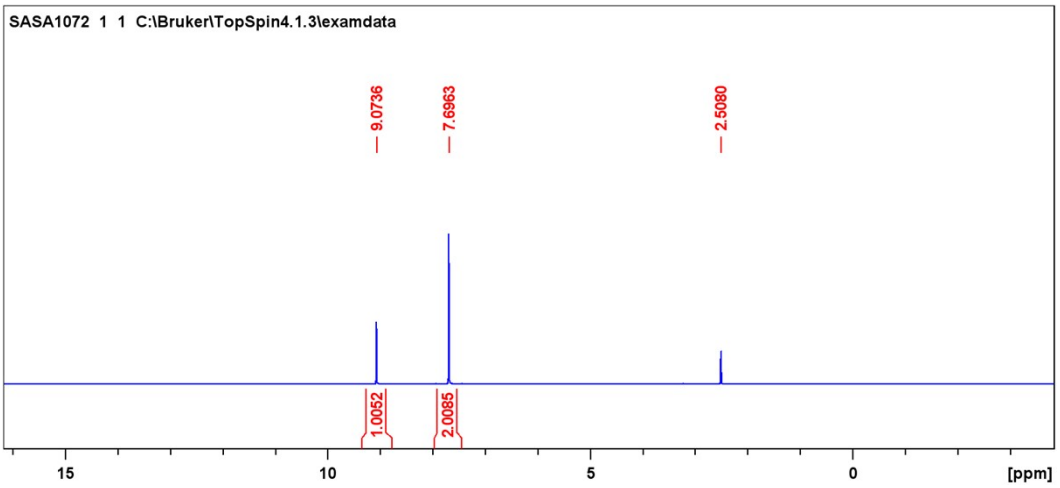

Figure S12 ^{1}HNMR of [Im][CF_3SO_3].

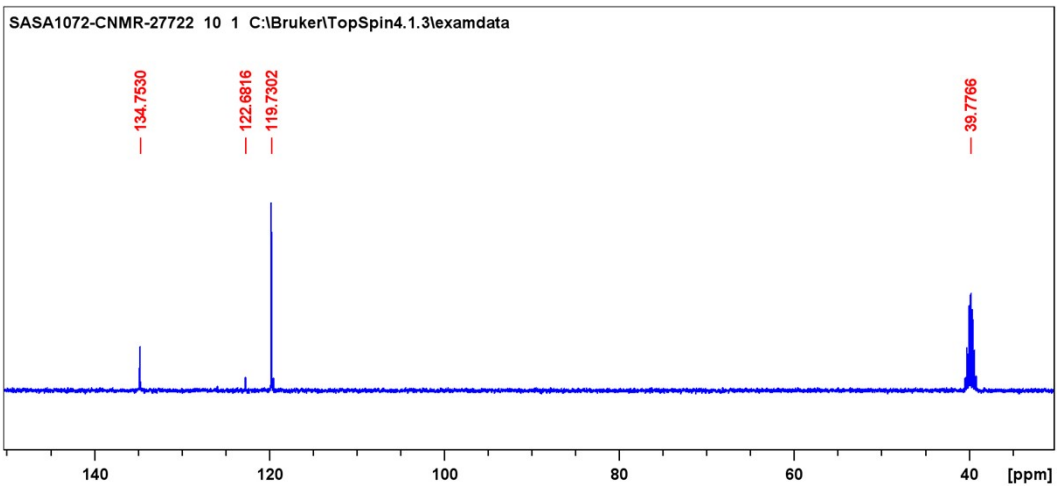

Figure S13 ^{13}CNMR of [Im][CF_3SO_3].

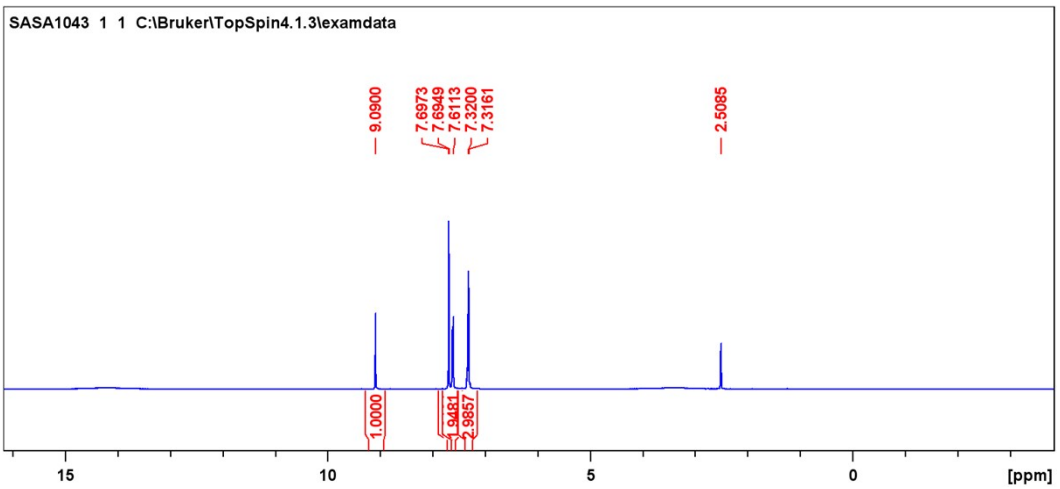

Figure S14 ^{1}HNMR of [Im][$C_6H_5SO_3$].

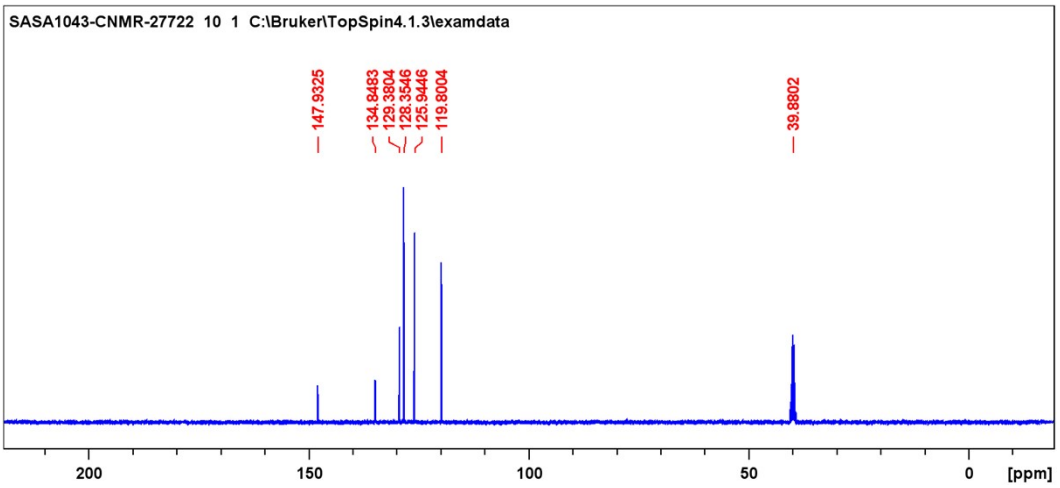

Figure S15 ^{13}CNMR of [Im][$C_6H_5SO_3$].

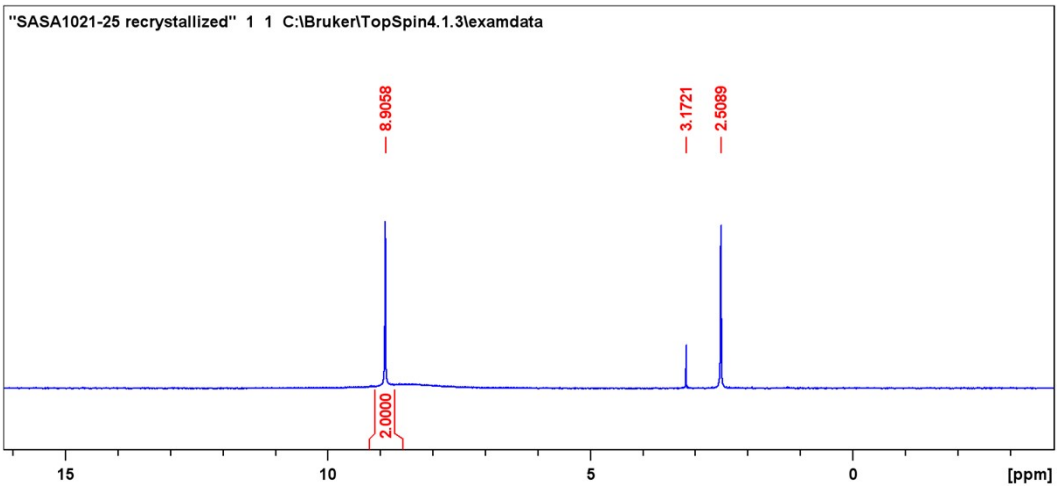

Figure S16 ^{1}HNMR of [Tri]Cl.

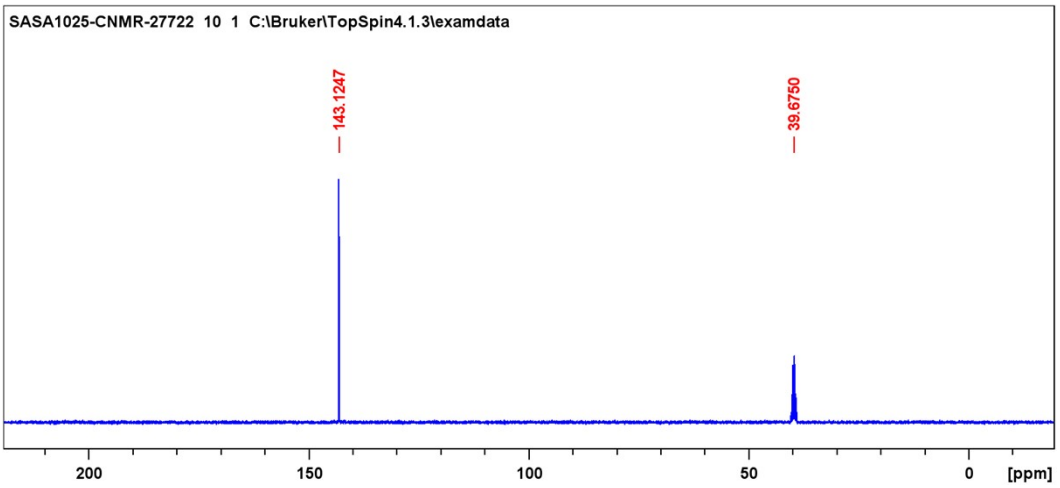

Figure S17^{13}CNMR of [Tri]Cl.

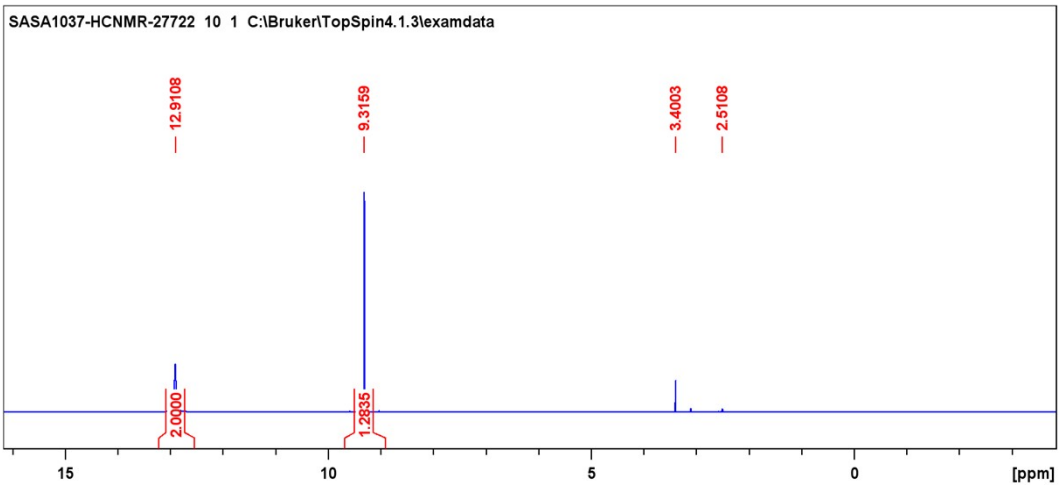

Figure S18 ^{1}HNMR of [Tri][HSO_4].

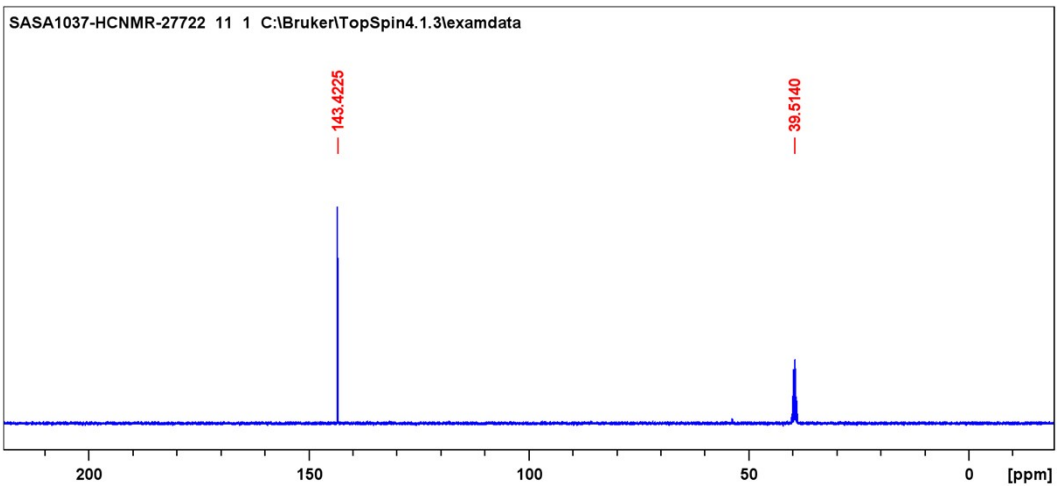

Figure S19 ^{13}CNMR of [Tri][HSO_4].

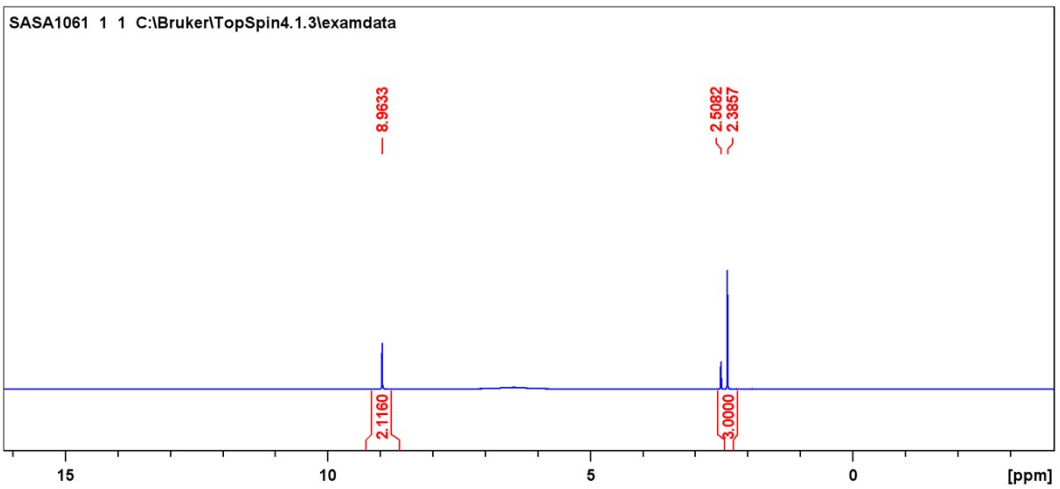

Figure S 20 ^{1}HNMR of [Tri][CH_3SO_3].

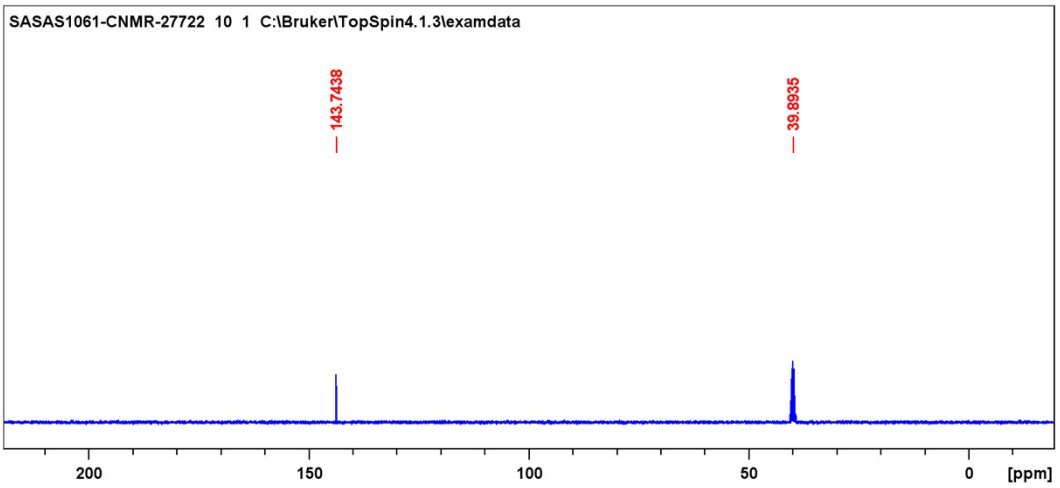

Figure S 21 ^{13}CNMR of [Tri][CH_3SO_3].

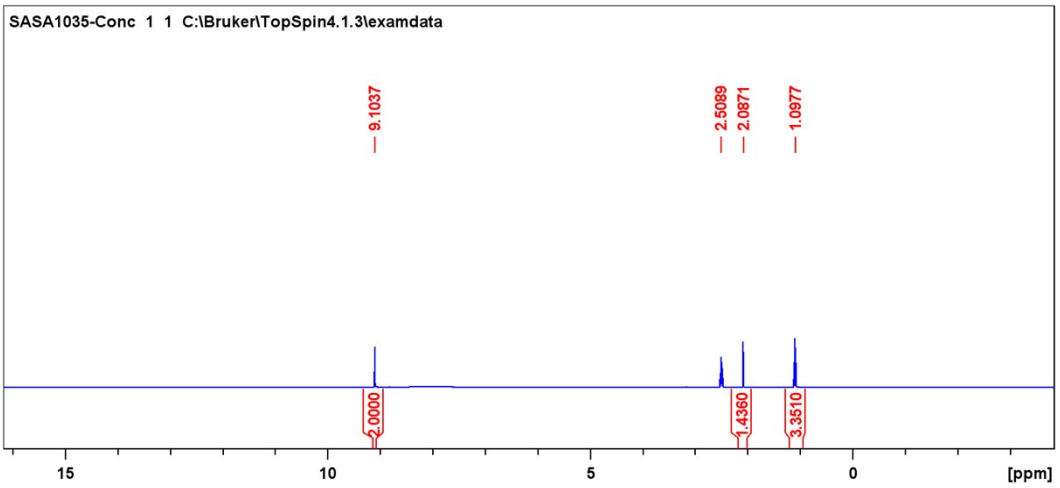

Figure S 22 ^{1}HNMR of [Tri][$C_2H_5SO_3$].

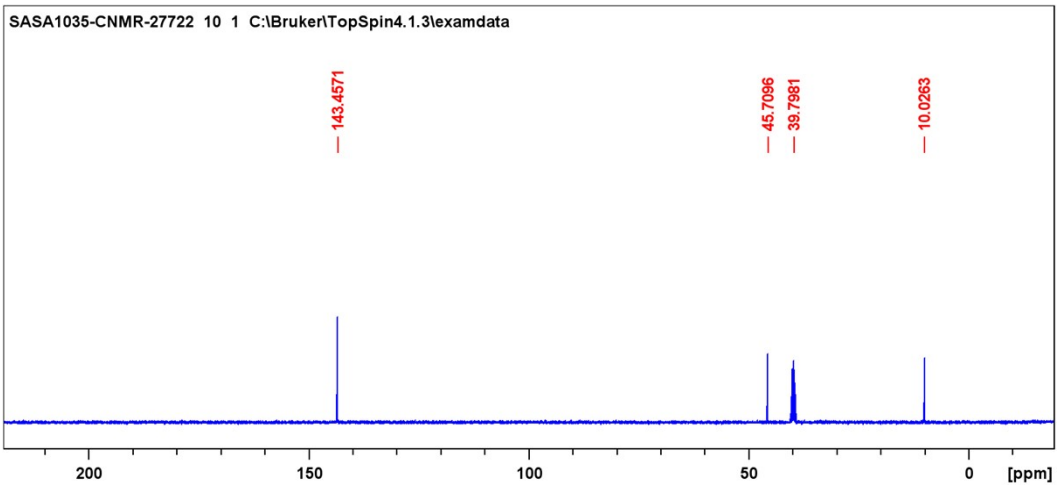

Figure S 23 ^{13}CNMR of [Tri][$C_2H_5SO_3$].

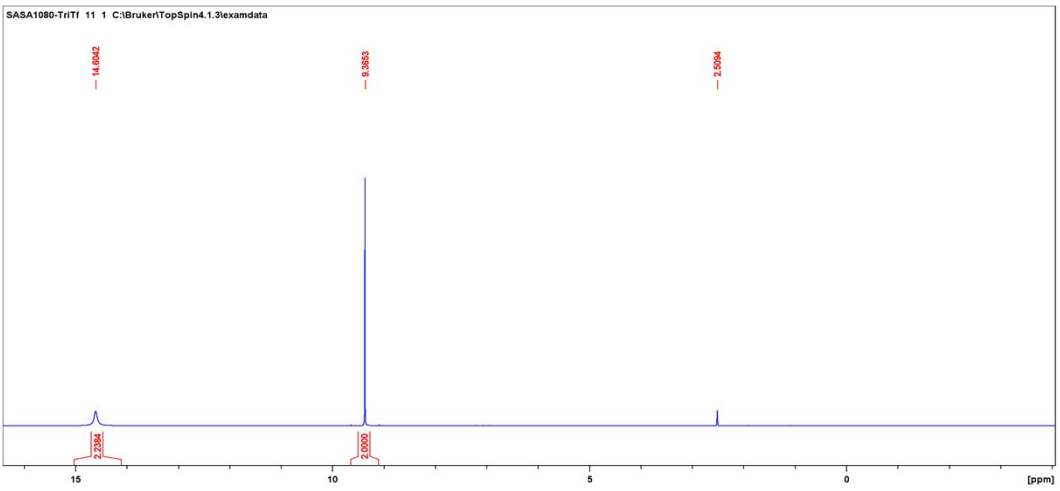

Figure S 24 ^{1}HNMR of [Tri][CF_3SO_3].

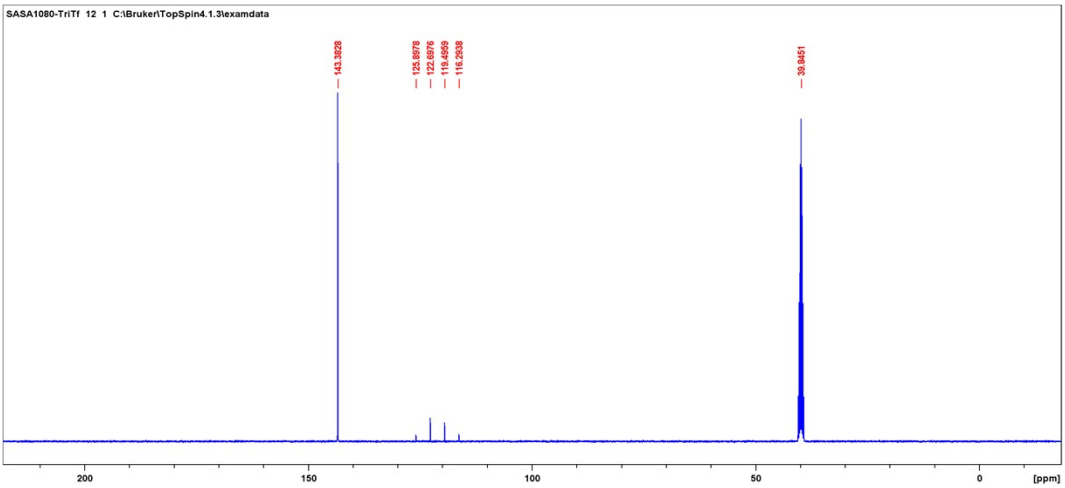

Figure S 25 ^{13}CNMR of [Tri][CF_3SO_3].

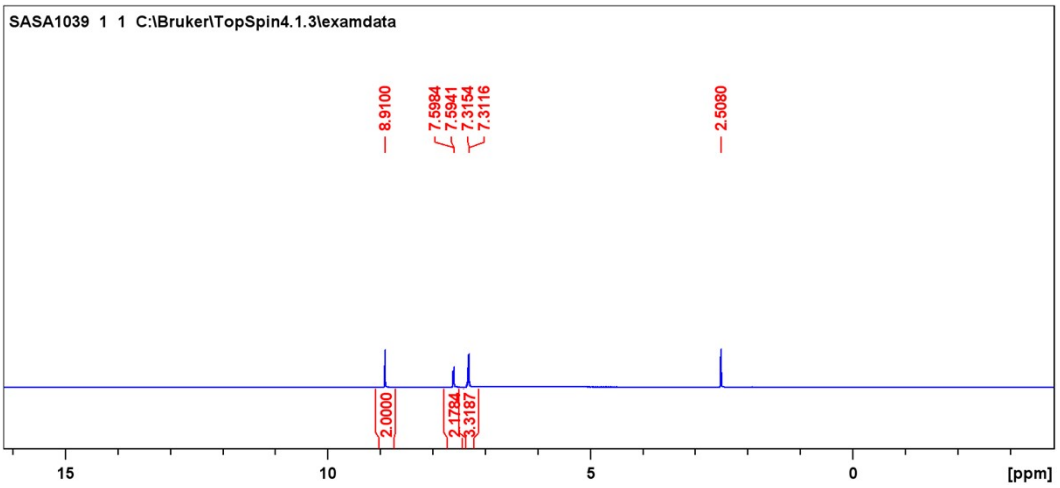

Figure S 26 ^{1}HNMR of [Tri][$C_6H_5SO_3$].

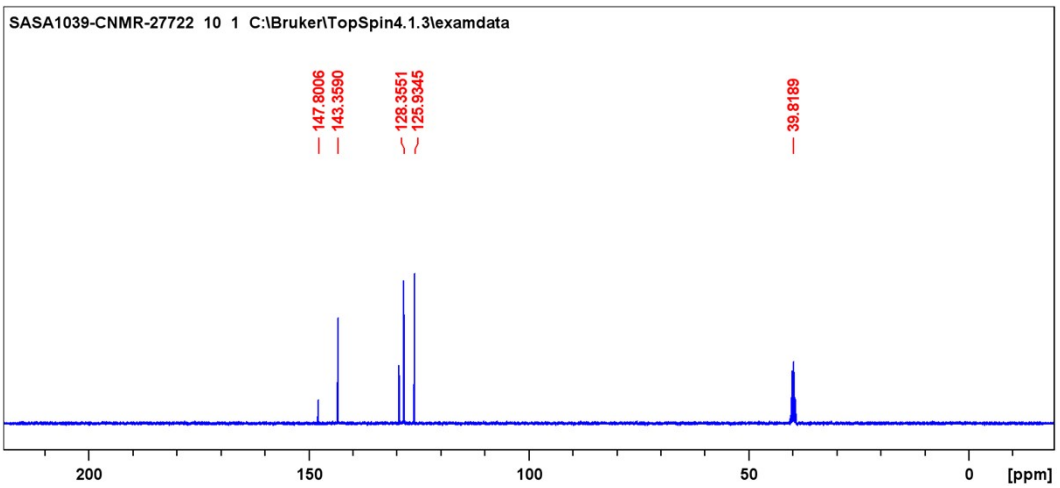

Figure S 27 ^{13}CNMR of [Tri][$C_6H_5SO_3$].

.

4.0 Single Crystal X-ray crystallography

Table S 1 Crystallographic structure data from literature obtained through Cambridge crystallographic Data Centre (CCDC).

Material	**CCDC database identifier**	**CCDC deposition number**	**Space group**	**a (Å)**	**b (Å)**	**c (Å)**	**α (°)**	**β (°)**	**γ (°)**	**ρ calc g.cm^{-3}**	**T, K**
[Im][CH_3SO_3][3]	JANCEK	2083427	Pbca (61)	8.0054(4)	11.1571 (8)	16.1757(8)	90	90	90	1.510	293
[Im][$C_2H_5SO_3$][3]	JANCIO	2083428	C2/c (15)	12.2768(6)	10.0322(5)	13.7525(7)	90	99.640(5)	90	1.418	293
[Pzy][HSO_4][4]	GAHYOH	1917638	$P2_1/c$ (14)	4.69440 (10)	8.9202 (2)	15.0248(3)	90	90.058	90	1.753	123
[Pzy][CH_3SO_3][4]	GAHYUN	1917639	$P2_1/c$ (14)	8.374(2)	7.610(2)	10.792(3)	90	90.011	90	1.591	123
[Pzy][CF_3SO_3][4]	GAHZAU	1917640	$P2_1/m$ (11)	5.2654 (2)	8.6830 (3)	9.0714 (3)	90	100.724(4)	90	1.778	173
[Pzy][$C_2H_5SO_3$][4]	GAHZEY	1917641	C c	12.82670(10)	9.5450(10)	13.27910(10)	90	98.7860	90	1.473	123
[Pzy][$C_6H_5SO_3$][4]	GAHZIC	1917642	$P2_1/c$ (14)	10.52760 (10)	8.36200 (10)	11.31660(10)	90	91.2050	90	1.509	123
[Pzy][Cl][5]	NUZKID	771215	$P2_1/n$ (14)	8.3797(7)	7.3935 (8)	8.7051(7)	90	114.398(5)	90	1.414	100
[Tri]Cl[6]	QULVEY	162785	$P2_1/n$ (14)	9.438(2)	8.683(2)	11.173 (2)	90	95.81(3)	90	1.539	297
[Tri][CH_3SO_3][7]	ITAFUF	804598	$P2_1/c$ (14)	5.4497 (4)	7.4823(7)	16.7814 (13)	90	95.212 (8)	90	1.610	153

Table S 2 Crystal structure and refinement data for imidazolium salts.

Identification code	**[Im]Cl**	**[Im][CF_3SO_3]**	**[Im][HSO_4]**	**[Im][$C_6H_5SO_3$]**
CCDC identifier	2313263	2313285	2313262	2313261
Empirical formula	$C_{48}H_{80}Cl_{16}N_{32}$	$C_4H_5F_3N_2O_3S$	$C_3H_6N_2O_4S$	$C_9H_{10}N_2O_3S$
Formula weight/g.mol^{-1}	1672.627	218.16	166.16	226.25
Temperature/K	123.15	123.15	123.15	123.15
Crystal system	Monoclinic	Tetragonal	Monoclinic	Orthorhombic
Space group	$P2_1/n$	$P4_32_12$	$P2_1/c$	Pbca
a/Å	15.0246(1)	8.11650(10)	4.49971(6)	8.16640(10)
b/Å	16.2945(2)	8.11650(10)	9.01283(13)	11.34490(10)
c/Å	16.7296(2)	24.8628(4)	15.7094(2)	21.5878(2)
α/°	90	90	90	90
β/°	107.861(1)	90	90.6000(12)	90
γ/°	90	90	90	90
Volume/Å^3	3898.31(8)	1637.90(5)	637.060(16)	2000.04 (4)
Z	2	8	4	8
ρ calc/g.cm^{-3}	1.425	1.769	1.732	1.503
μ/mm^{-1}	5.630	3.949	4.273	2.817
F(000)	1744.2	880.0	344.0	944.0
Crystal size/mm^3	0.028 × 0.037×0.267	0.062×0.072×0.206	0.024 × 0.039× 0.236	0.058×0.119×0.213
Radiation	Cu Kα (λ = 1.54184)	Cu Kα (λ = 1.54184)	CuKα (λ = 1.54184)	CuKα (λ = 1.54184)
2θ range for data collection/°	6.92 to 160.3	11.468 to 160.47	11.266 to 160.73	8.192 to 160.546
Index ranges	-18 ≤ h ≤ 10, -20 ≤ k ≤ 19, -21 ≤ l ≤ 21	-9 ≤ h ≤ 10, -9 ≤ k ≤ 9, -31 ≤ l ≤ 30	-5 ≤ h ≤ 4, -9 ≤ k ≤ 11, -20 ≤ l ≤ 19	-9 ≤ h ≤ 10, -9 ≤ k ≤ 14, -27 ≤ l ≤ 21
Reflections collected	42260	8852	7009	11327
Independent reflections	8330 [R_{int} = 0.0472, R_{sigma} = 0.0353]	1743 [R_{int} = 0.0414, R_{sigma} = 0.0318]	1361 [R_{int} = 0.0313, R_{sigma} = 0.0210]	2151 [R_{int} = 0.0220, R_{sigma} = 0.0163]
Data/restraints/parameters	8330/16/433	1743/0/126	1361/0/103	2151/0/70
Goodness of fit on F2	1.023	1.097	1.055	1.069
Final R indexes [I>=2σ(I)]	R_1 = 0.0426, wR_2 = 0.1138	R_1 = 0.0431, wR_2 = 0.1155	R_1 = 0.0290, wR_2 = 0.0789	R_1 = 0.0442, wR_2 = 0.1101
Final R indexes (all data)	R_1 = 0.0482, wR_2 = 0.1175	R_1 = 0.0445, wR_2 = 0.1168	R_1 = 0.0296, wR_2 = 0.0793	R_1 = 0.0453, wR_2 = 0.1109
Largest diff peak/hole/e Å^{-3}	0.74/-0.67	0.62/-0.42	0.23/-0.55	0.68/-0.65
Flack parameter		0.001(13)		

Table S 3 Crystal structure and refinement details of 1,2,4-triazolium salts.

Identification code	**[Tri][HSO_4]**	**[Tri][$C_2H_5SO_3$]**	**[Tri][CF_3SO_3]**	**[Tri][$C_6H_5SO_3$]**
CCDC identifier	2313265	2313266	2313267	2313264
Empirical formula	$C_2H_5N_3O_4S$	$C_4H_9N_3O_3S$	$C_3H_4F_3N_3O_3S$	$C_8H_9N_3O_3S$
Formula weight/g.mol^{-1}	167.15	179.20	219.15	227.24
Temperature/K	123.15	123.15	123.15	123.15
Crystal system	Monoclinic	Triclinic	Triclinic	Monoclinic
Space group	$P2_1/n$	P-1	P-1	$P2_1/c$
a/Å	6.50504(8)	5.16580(10)	5.28976(18)	5.31130(10)
b/Å	5.29352(7)	11.1478(2)	8.2702(3)	22.0575(4)
c/Å	16.91686(18)	13.9104(2)	8.6996(2)	8.18530(10)
α/°	90	81.6110(10)	88.420(3)	90
β/°	91.1450(10)	82.7060(10)	88.373(3)	92.4580(10)
γ/°	90	77.9530(10)	88.468(3)	90
Volume/Å^3	582.408(12)	771.17(2)	380.16(2)	958.06(3)
Z	4	4	2	4
ρ calc/g.cm^{-3}	1.906	1.543	1.915	1.575
μ/mm^{-1}	4.731	3.510	4.297	2.975
F(000)	344.0	376.0	220.0	472.0
Crystal size/mm^3	0.107×0.156×0.242	0.191×0.208×0.277	0.090 × 0.159 × 0.488	0.018×0.030×0.214
Radiation	CuKα (λ = 1.54184)	CuKα (λ = 1.54184)	CuKα (λ = 1.54184)	CuKα (λ = 1.54184)
2θ range for data collection	10.46 to 160.492	8.172 to159.832	10.176 to 160.316	8.016 to 159.454
Index ranges	-5 ≤ h ≤ 8, -6 ≤ k ≤ 6, -21 ≤ l ≤ 21	-6 ≤ h ≤ 6, -14 ≤ k ≤ 13, -17 ≤ l ≤ 17	-6 ≤ h ≤ 6, -8 ≤ k ≤ 10, -10 ≤ l ≤ 11	-6 ≤ h ≤ 6, -27 ≤ k ≤ 28, -7 ≤ l ≤ 10
Reflections collected	6348	30549	8004	9964
Independent reflections	1251 [R_{int} = 0.0191, R_{sigma} = 0.0133]	3301 [R_{int} = 0.0423, R_{sigma} = 0.0171]	1616 [R_{int} = 0.0452, R_{sigma} = 0.0302]	2046 [R_{int} = 0.0354, R_{sigma} = 0.0268]
Data/restraints/parameter	1251/0/103	3301/0/218	1616/0/126	2046/6/202
Goodness of fit on F2	1.105	1.150	1.082	1.061
Final R indexes [I>=2σ(I)]	R_1 = 0.0273, wR_2 = 0.0759	R_1 = 0.0322, wR_2 = 0.1041	R_1 = 0.0397, wR_2 = 0.1107	R_1 = 0.0567, wR_2 = 0.1533
Final R indexes (all data)	R_1 = 0.0274, wR_2 = 0.0760	R_1 = 0.0337, wR_2 = 0.1053	R_1 = 0.0413, wR_2 = 0.1123	R_1 = 0.0592, wR_2 = 0.1564
Largest diff peak/hole/e Å^{-3}	0.21/-0.52	0.31/-0.48	0.82/-0.58	0.93/-0.51
Flack Parameter	-	-	-	-

4.1 Chlorides

a) **b)** **c)**

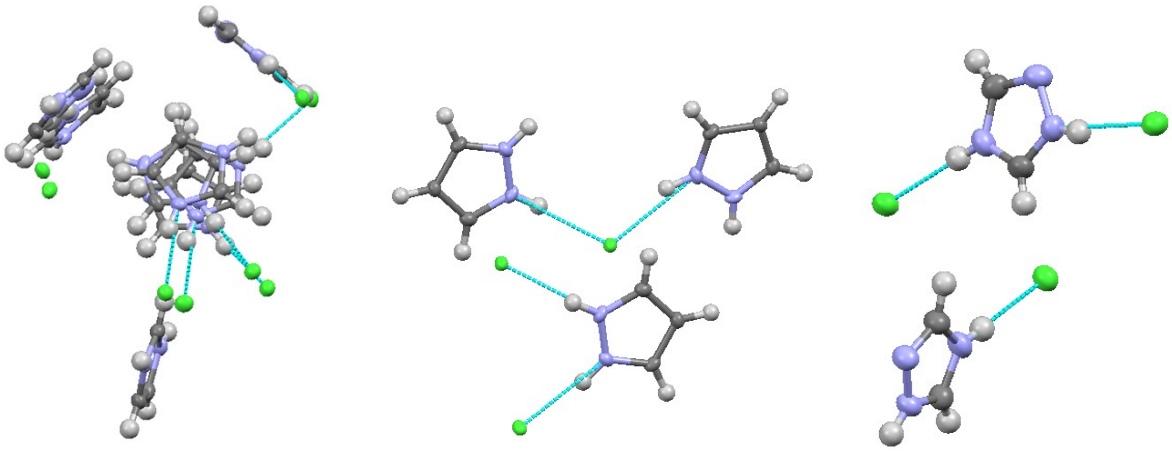

*Figure S 28 Crystallographic determined structure of [Im]Cl **(a)**, [Pzy]Cl **(b)**, [Tri]Cl **(c)** Nitrogen is shown in purple color and chloride ions are shown in green. The hydrogen atoms are shown in light grey color and hydrogen bonds are represented by dotted turquoise line.*

a) **b)** **c)**

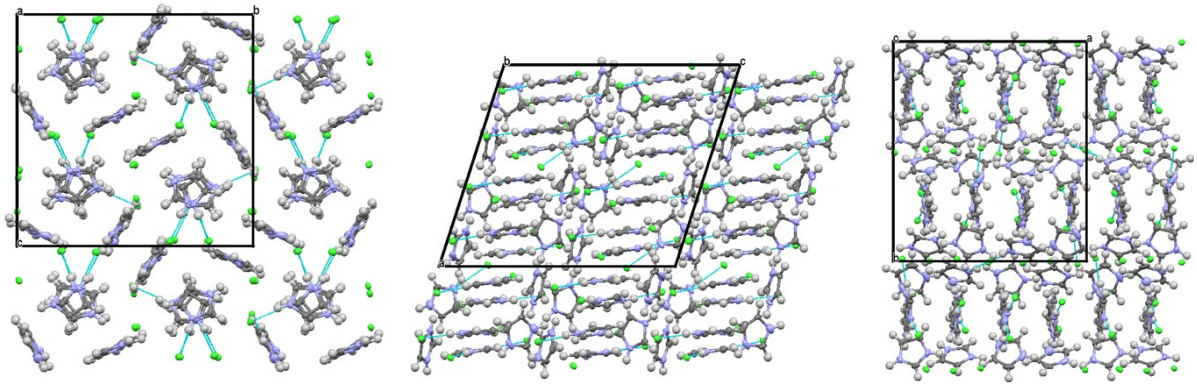

*Figure S 29 Crystal packing of [Im]Cl down the a **(a)**, b **(b)**, and c **(c)** axis. 1.5 unit cells are packed along each axis. Hydrogen bonds are represented by broken turquoise lines.*

a) **b)** **c)**

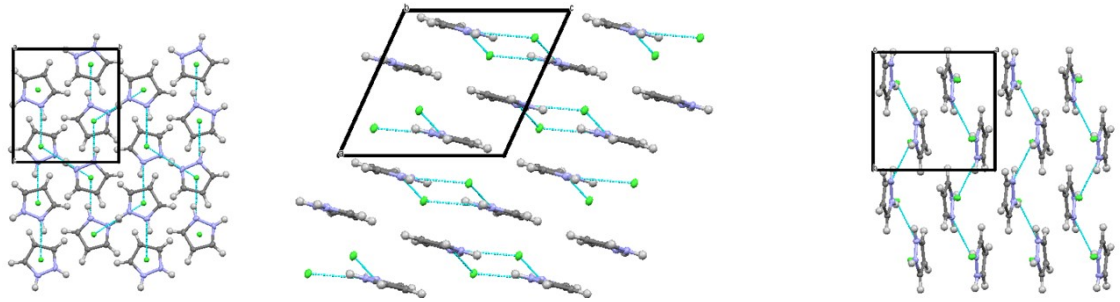

*Figure S 30 Crystal packing of [Pzy]Cl down the a **(a)**, b **(b)**, and c **(c)** axis. Two unit cells are packed along each axis. Hydrogen bonds are represented by broken turquoise lines.*

a) **b)** **c)**

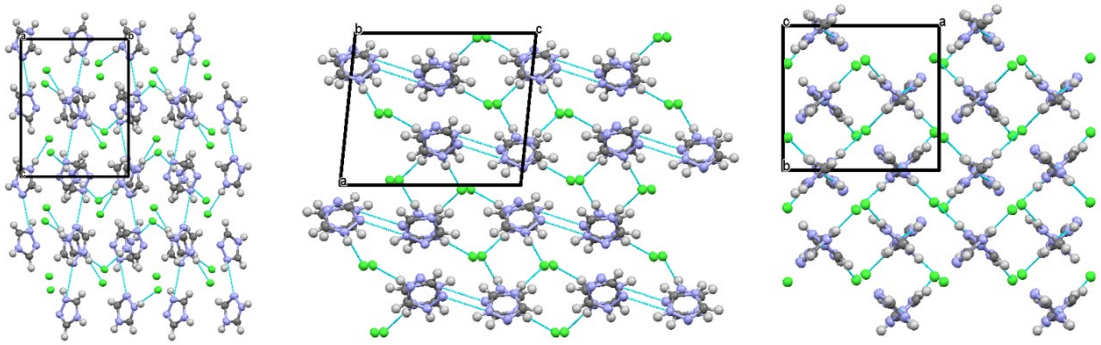

*Figure S 31 Crystal packing of [Tri]Cl chloride down the a **(a)**, b **(b)**, and c **(c)** axis. Two unit cells are packed along each axis. Hydrogen bonds are represented by turquoise broken lines. Two unit cells are packed along each axis. The hydrogen bond is represented by dotted turquoise line.*

4.2 Mesylates

a) **b)** **c)**

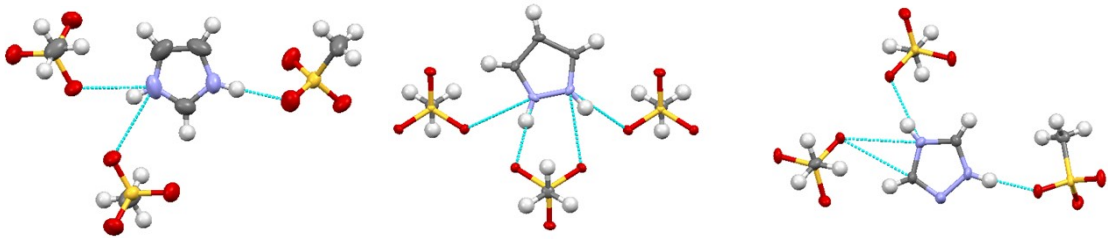

*Figure S 32 Crystallographic determined structure of [Im][CH_3SO_3] **(a)**, [Pzy][CH_3SO_3] **(b)**, [Im][CH_3SO_3] **(c)** Nitrogen is shown in purple color and chloride ions are shown in green. The hydrogen atoms are shown in light grey color and hydrogen bonds are represented by dotted turquoise line.*

a) **b)** **c)**

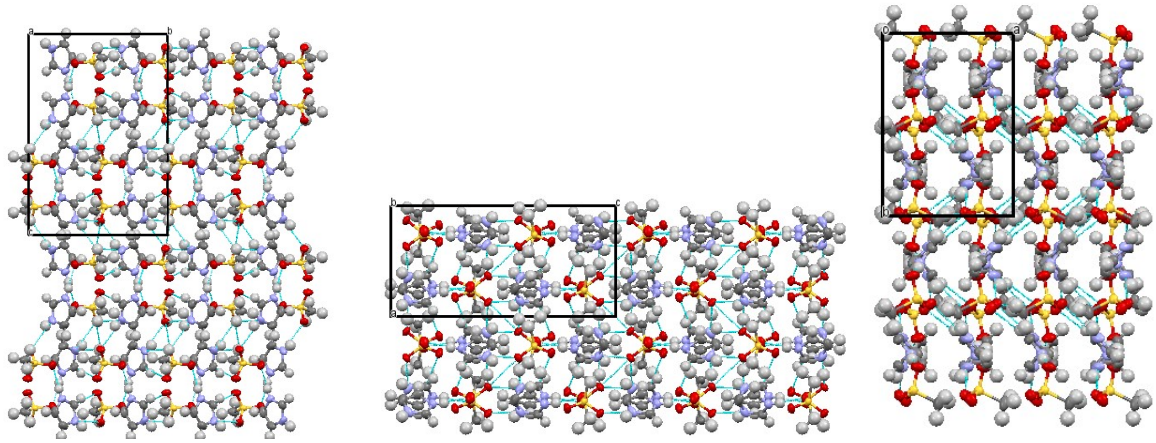

Figure S 33 Crystal packing of [Im][CH_3SO_3] down the a (a), b (b), and c (c) axis. Two unit cells are packed along each axis. Hydrogen bonds are represented by turquoise broken lines.

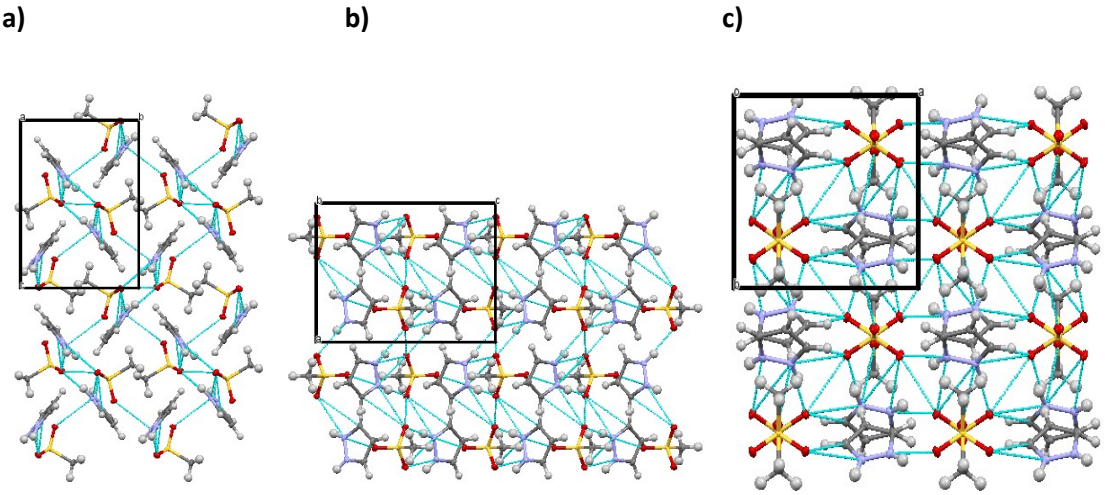

Figure S 34 Crystal packing of [Pzy][CH_3SO_3] down the a (a), b (b), and c (c) axis. Two unit cells are packed along each axis. Hydrogen bonds are represented by turquoise broken lines.

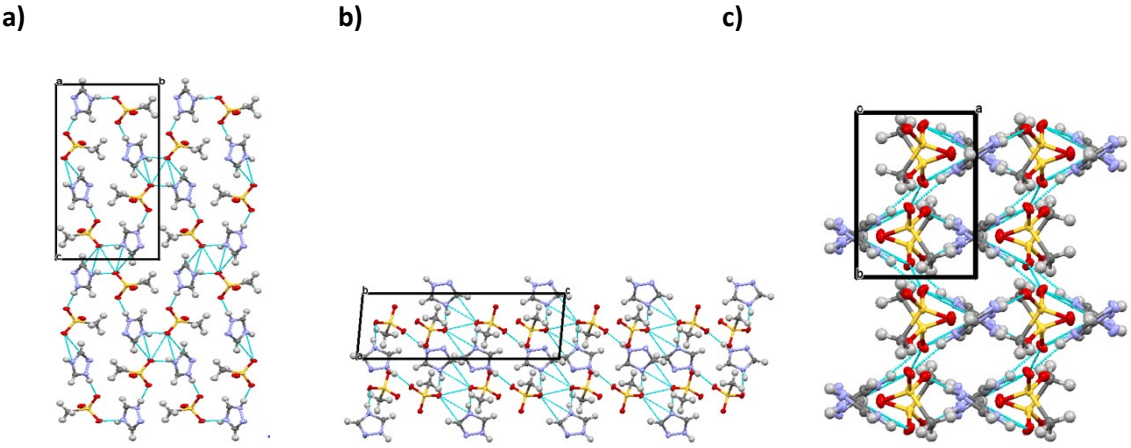

Figure S 35 Crystal packing of [Tri][CH_3SO_3] down the a (a), b (b), and c (c) axis. Two unit cells are packed along each axis. Hydrogen bonds are represented by turquoise broken lines.

4.3 Ethanesulfonate

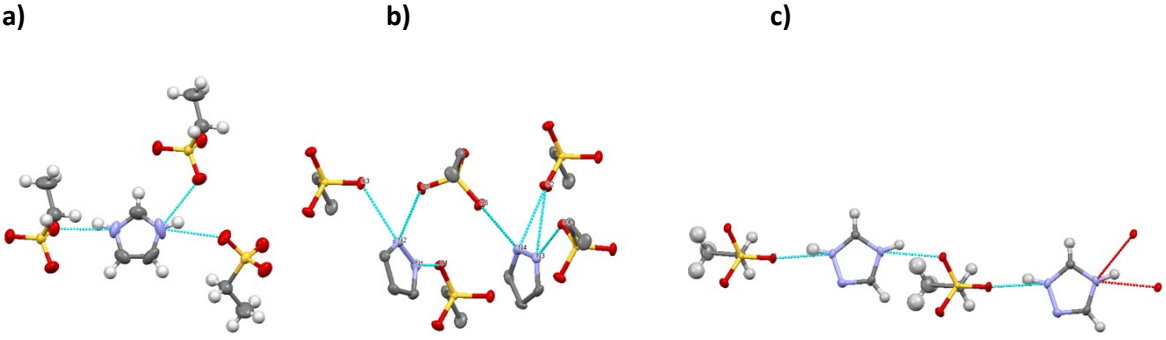

*Figure S 36 Crystallographic determined structure of [Im][$C_2H_5SO_3$] **(a)**, [Pzy] [$C_2H_5SO_3$] **(b)**, [Tri] [$C_2H_5SO_3$] **(c)** Nitrogen is shown in purple color and chloride ions are shown in green. The hydrogen atoms are shown in light grey color and hydrogen bonds are represented by dotted turquoise line.*

a) **b)** **c)**

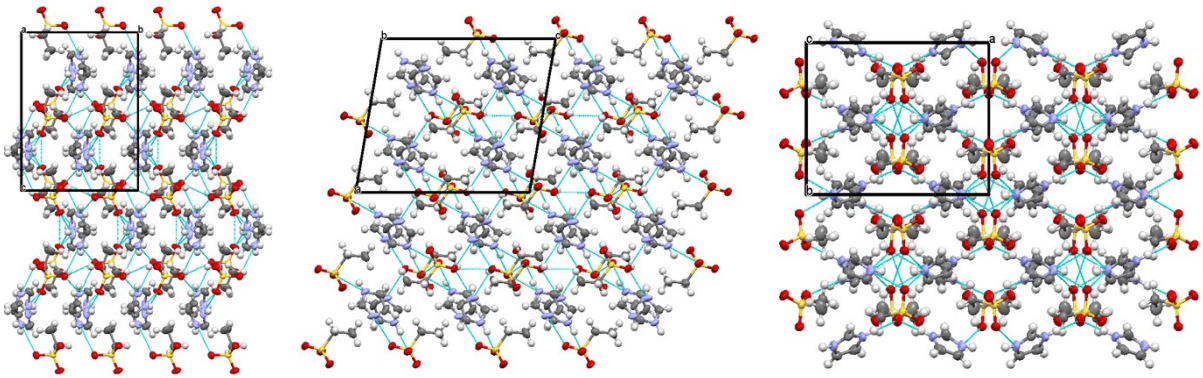

Figure S 37 Crystal packing of [Im][$C_2H_5SO_3$] down the a (a), b (b), and c (c) axis. Two unit cells are packed along each axis. Hydrogen bonds are represented by turquoise broken lines.

a) **b)** **c)**

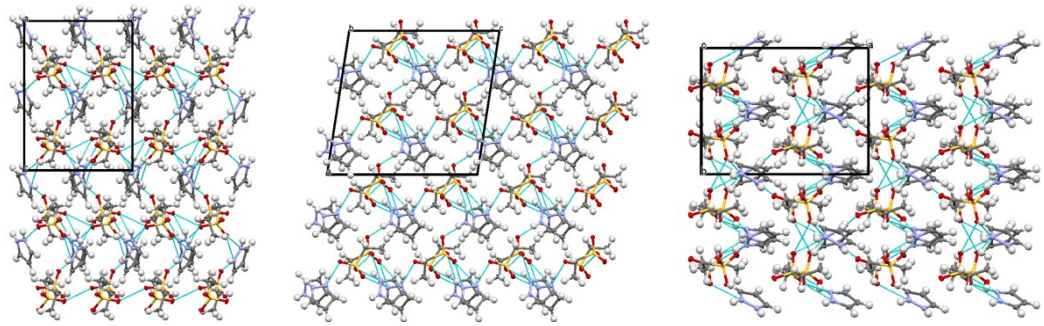

Figure S 38 Crystal packing of [Pzy][$C_2H_5SO_3$] down the a (a), b (b), and c (c) axis. Two unit cells are packed along each axis. Hydrogen bonds are represented by turquoise broken lines.

a) **b)** **c)**

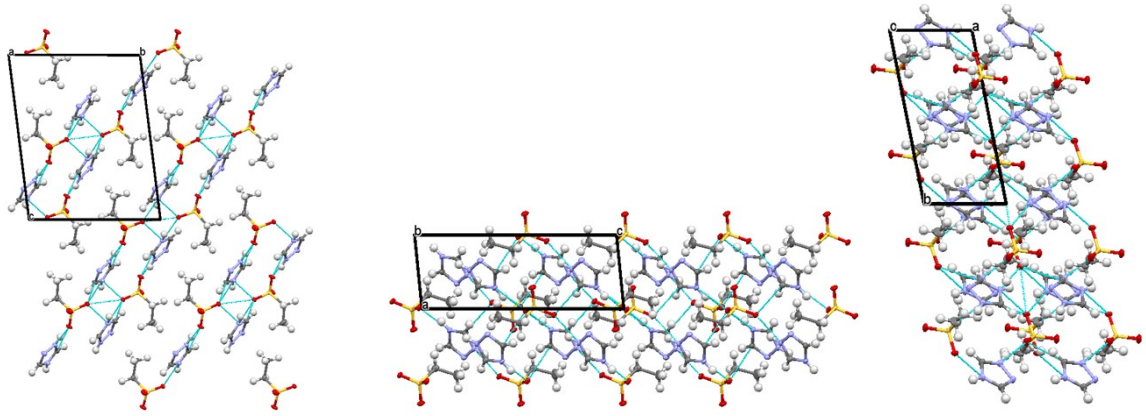

Figure S 39 Crystal packing of [1,2,4-Tri][$C_2H_5SO_3$] down the a (a), b (b), and c (c) axis. Two unit cells are packed along each axis. Hydrogen bonds are represented by turquoise broken lines.

4.4 Triflate

a) **b)** **c)**

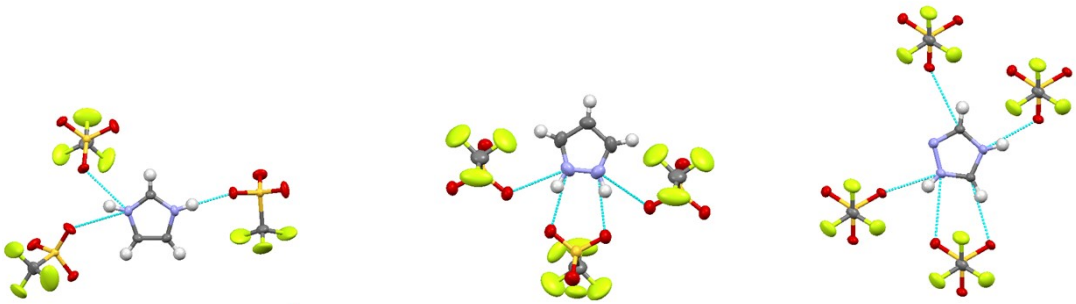

*Figure S 40 Crystallographic determined structure of [Im][CF_3SO_3] **(a)**, [Pzy][CF_3SO_3] **(b)**, [Im][CF_3SO_3] **(c)** Nitrogen is shown in purple color, fluorine atoms are shown in yellow, oxygen atoms are shown in red and the hydrogen atoms are shown in light grey color and hydrogen bonds are represented by dotted turquoise broken line.*

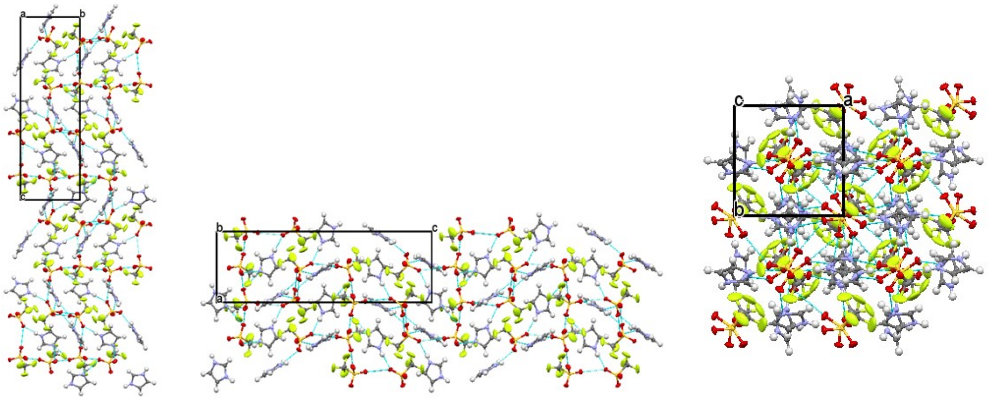

Figure S 41 Crystal packing of [Im][CF_3SO_3] down the a (a), b (b), and c (c) axis. Three unit cells are packed along each axis. Fluorine atoms are shown by yellow color, oxygen atoms by red color and hydrogen bonds are represented by turquoise broken lines.

a) **b)** **c)**

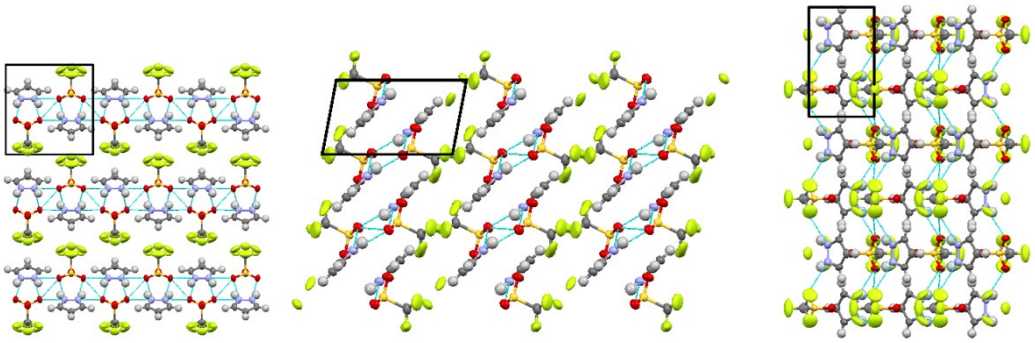

Figure S 42 Crystal packing of [Pzy][CF_3SO_3] down the a (a), b (b), and c (c) axis. Three unit cells are packed along each axis. Fluorine atoms are shown by yellow color, oxygen atoms by red color and hydrogen bonds are represented by turquoise broken lines.

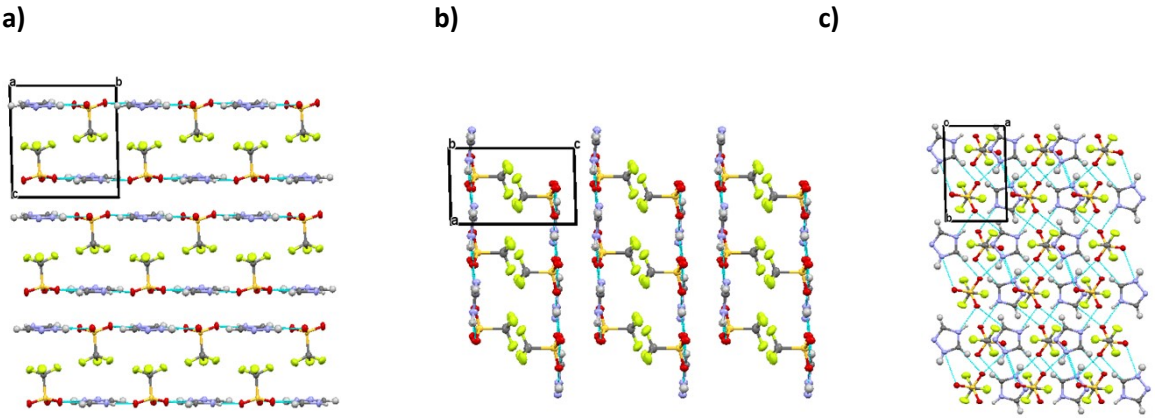

Figure S 43 Crystal packing of [Tri][CF_3SO_3] down the a (a), b (b), and c (c) axis. Three unit cells are packed along each axis. Fluorine atoms are shown by yellow color, oxygen atoms by red color and hydrogen bonds are represented by turquoise broken lines.

4.5 Benzensulfonate

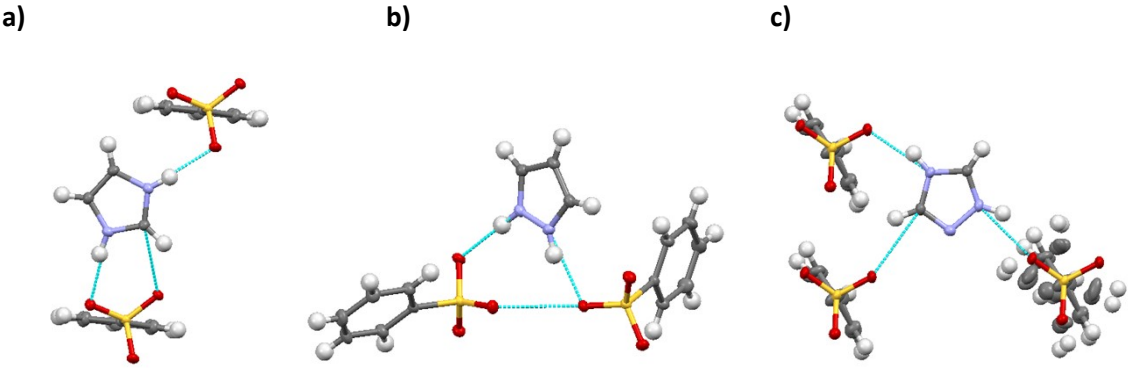

*Figure S 44 Crystallographic determined structure of [Im][$C_6H_5SO_3$] **(a)**, [Pzy] [$C_6H_5SO_3$] **(b)**, [1,2,4-Tri] [$C_6H_5SO_3$] **(c)** Nitrogen is shown in purple color, oxygen atoms are shown in red and the hydrogen atoms are shown in light grey color and hydrogen bonds are represented by dotted turquoise broken line.*

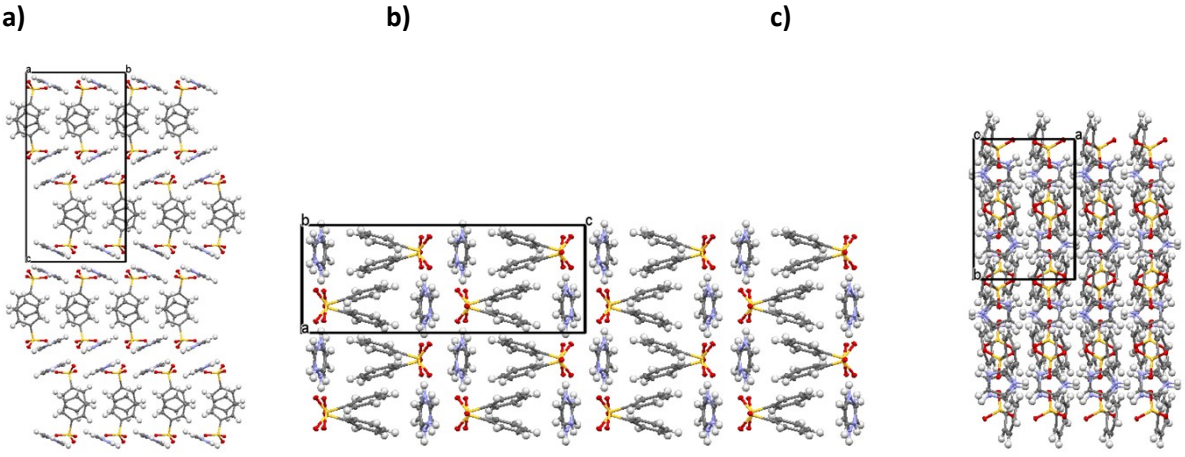

Figure S 45 Crystal packing of [Im][$C_6H_5SO_3$] down the a (a), b (b), and c (c) axis. 1.5 unit cells are packed along each axis. The oxygen atoms are shown by red color and hydrogen bonds are represented by turquoise broken lines.

a) **b)** **c)**

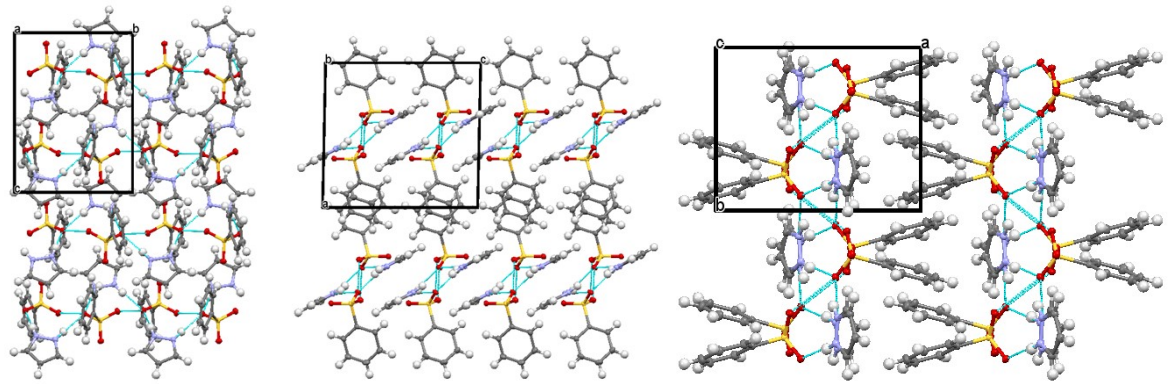

Figure S 46 Crystal packing of [Pzy][$C_6H_5SO_3$] down the a (a), b (b), and c (c) axis. 1.5 unit cells are packed along each axis. The oxygen atoms are shown by red color and hydrogen bonds are represented by turquoise broken lines.

a) **b)** **c)**

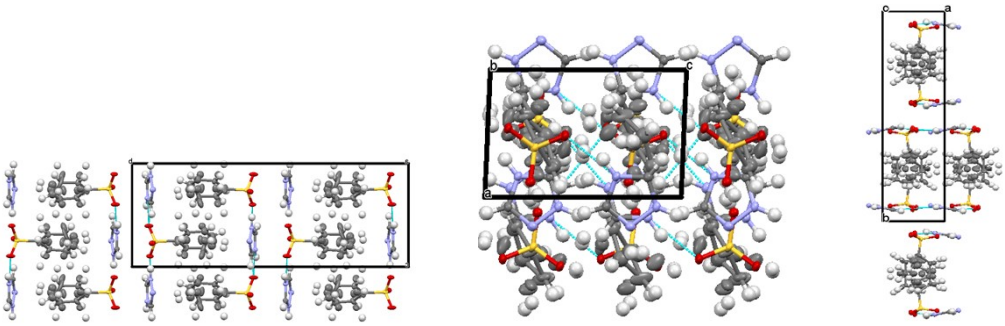

Figure S 47 Crystal packing of [Tri][$C_6H_5SO_3$] down the a (a), b (b), and c (c) axis. 1.5 unit cells are packed along each axis. The oxygen atoms are shown by red color and hydrogen bonds are represented by turquoise broken lines.

a) **b)** **c)**

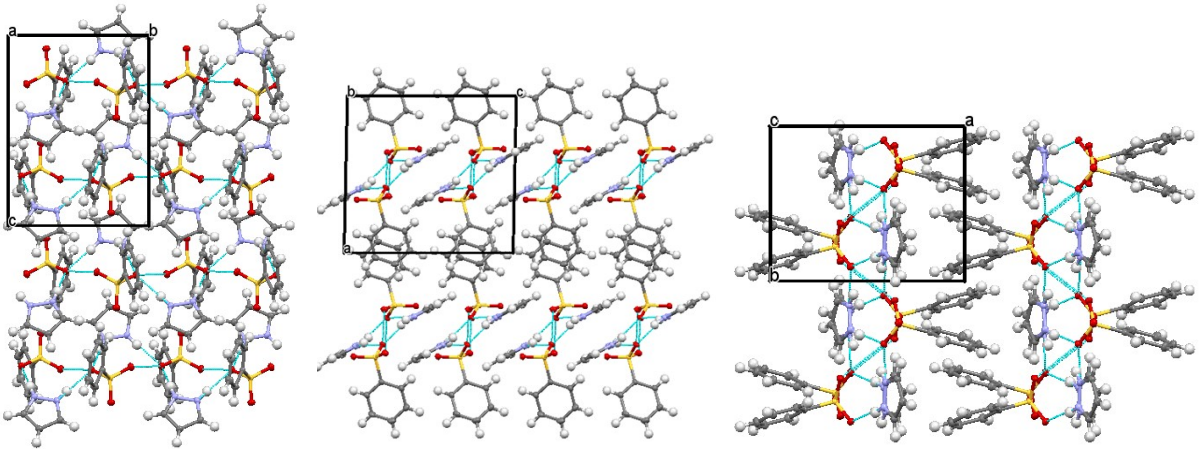

Figure S 48 Crystal packing of [Pzy][$C_6H_5SO_3$] down the a (a), b (b), and c (c) axis. Two unit cells are packed along each axis. Fluorine atoms are shown by yellow color, oxygen atoms by red color and hydrogen bonds are represented by turquoise broken lines.

4.6 Hydrogen sulfate

a) **b)** **c)**

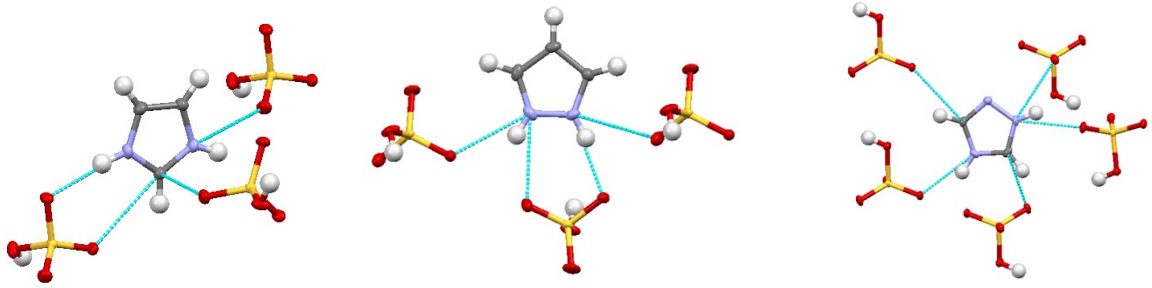

*Figure S 49 Crystallographic determined structure of [Im][$C_2H_5SO_3$] **(a)**, [Pzy] [$C_2H_5SO_3$] **(b)**, [Tri] [$C_2H_5SO_3$] **(c)** Nitrogen is shown in purple color and chloride ions are shown in green. The hydrogen atoms are shown in light grey color and hydrogen bonds are represented by dotted turquoise line.*

a) **b)** **c)**

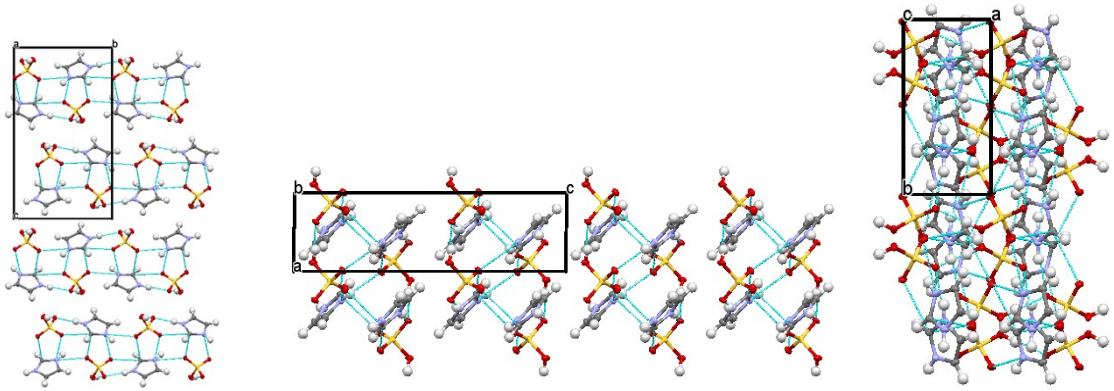

Figure S 50 Crystal packing of [Im][HSO_4] down the a (a), b (b), and c (c) axis. Two unit cells are packed along each axis. Fluorine atoms are shown by yellow color, oxygen atoms by red color and hydrogen bonds are represented by turquoise broken lines.

a) **b)** **c)**

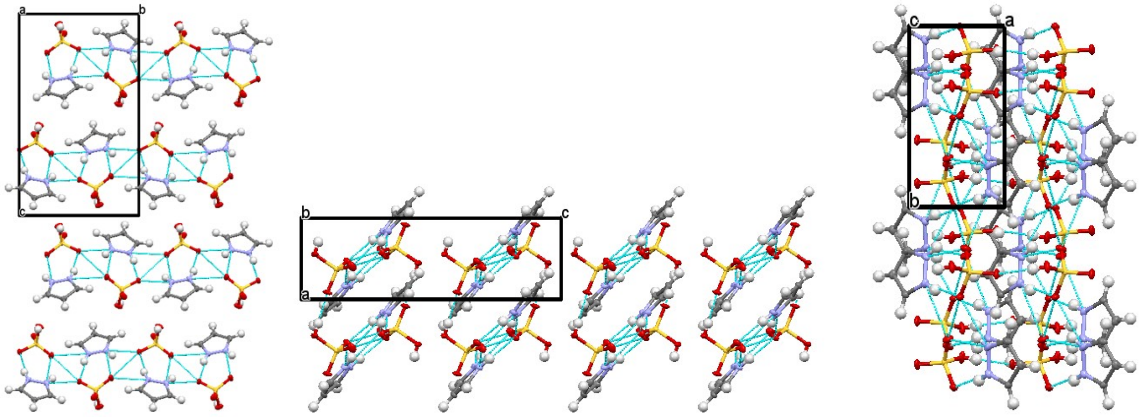

Figure S 51 Crystal packing of [Pzy][HSO_4] down the a (a), b (b), and c (c) axis. Two unit cells are packed along each axis. Fluorine atoms are shown by yellow color, oxygen atoms by red color and hydrogen bonds are represented by turquoise broken lines.

a) **b)** **c)**

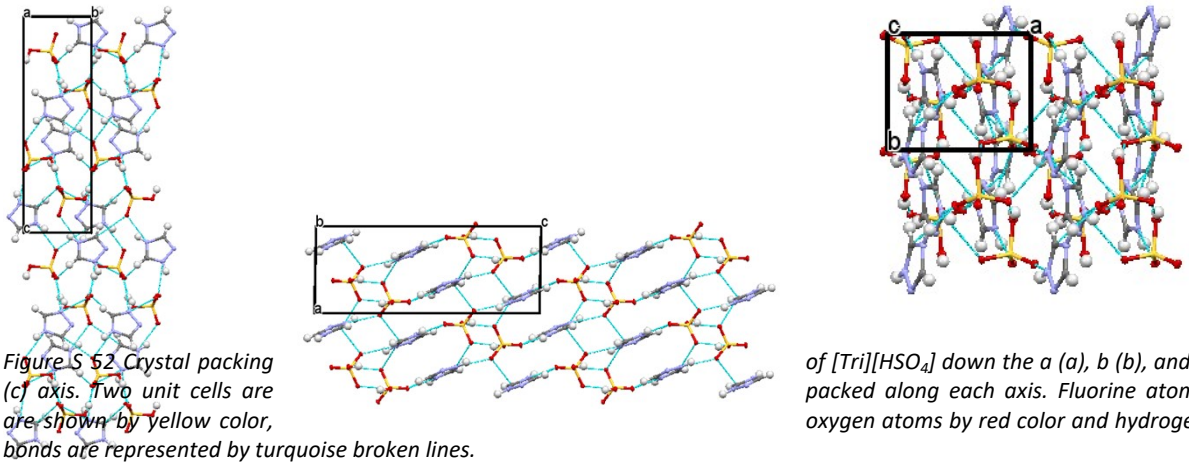

Figure S 52 Crystal packing of [Tri][HSO_4] down the a (a), b (b), and c (c) axis. Two unit cells are packed along each axis. Fluorine atoms are shown by yellow color, oxygen atoms by red color and hydrogen bonds are represented by turquoise broken lines.

5 Hirshfeld surface analysis

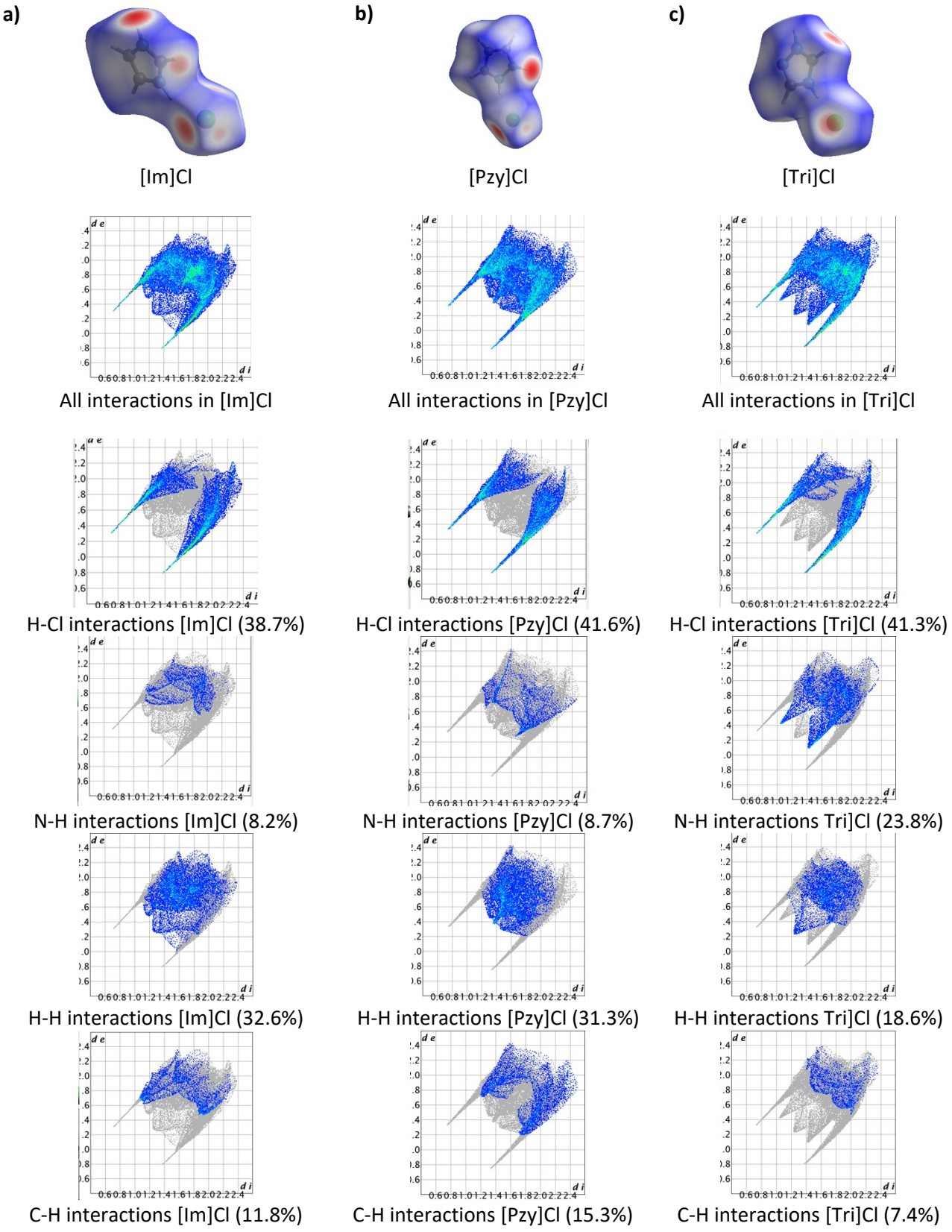

Figure S 53 Distribution of various intermolecular interactions over the Hirshfeld surface of [Im]Cl, [Pzy]Cl and [Tri]Cl (one ion pair was chosen for each salt).

a) **b)** **c)**

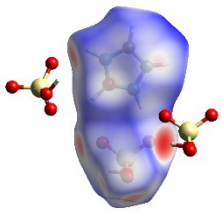

[Im][HSO_4]

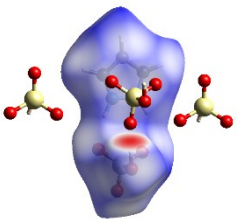

[Pzy][HSO_4]

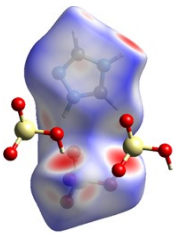

[Tri][HSO_4]

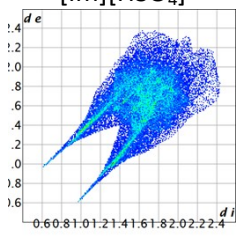

All interactions [Im][HSO_4]

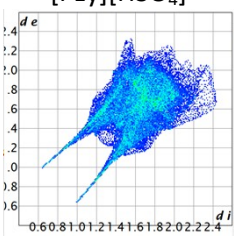

All interactions [Pzy][HSO_4]

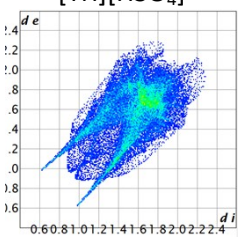

All interactions [Tri][HSO_4]

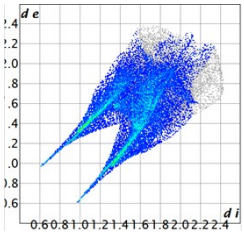

O-H interactions [Im][HSO_4] (58.4%)

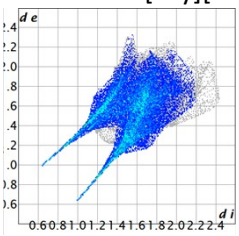

O-H interactions [Pzy][HSO_4] (54.5%)

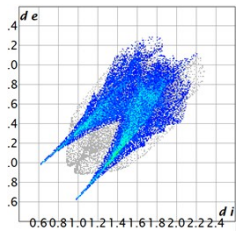

O-H interactions [Tri][HSO_4] (56%)

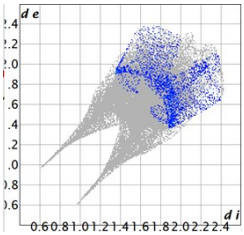

N-H interactions [Im][HSO_4] (4.3%)

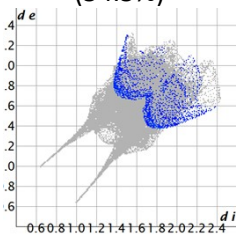

N-H interactions [Pzy][HSO_4] (4.4%)

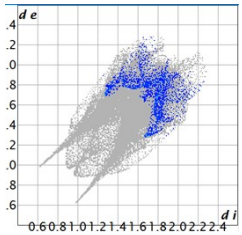

N-H interactions [Tri][HSO_4] (5%)

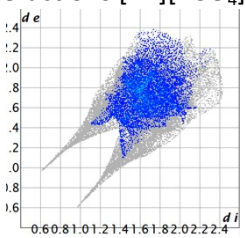

H-H interactions [Im][HSO_4] (19.1%)

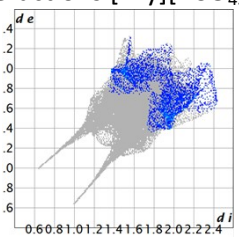

H-H interactions [Pzy][HSO_4] (20.9%)

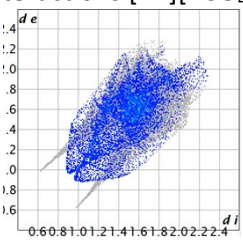

H-H interactions [Tri][HSO_4] (21%)

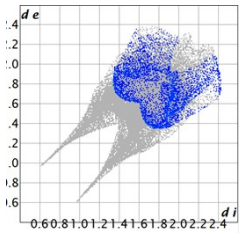

C-H interactions [Im][HSO_4] (9.4%)

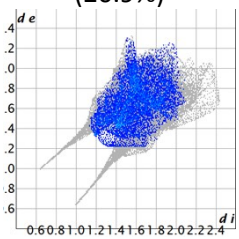

C-H interactions [Pzy][HSO_4] (8.8%)

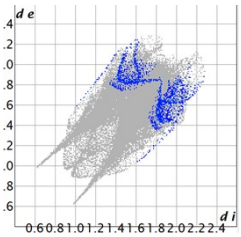

C-H interactions [Tri][HSO_4] (3.9%)

Figure S 54 Table S 4 Hirshfeld surface analysis of [Im][HSO_4], [Pzy][HSO_4], and [Tri][HSO_4].

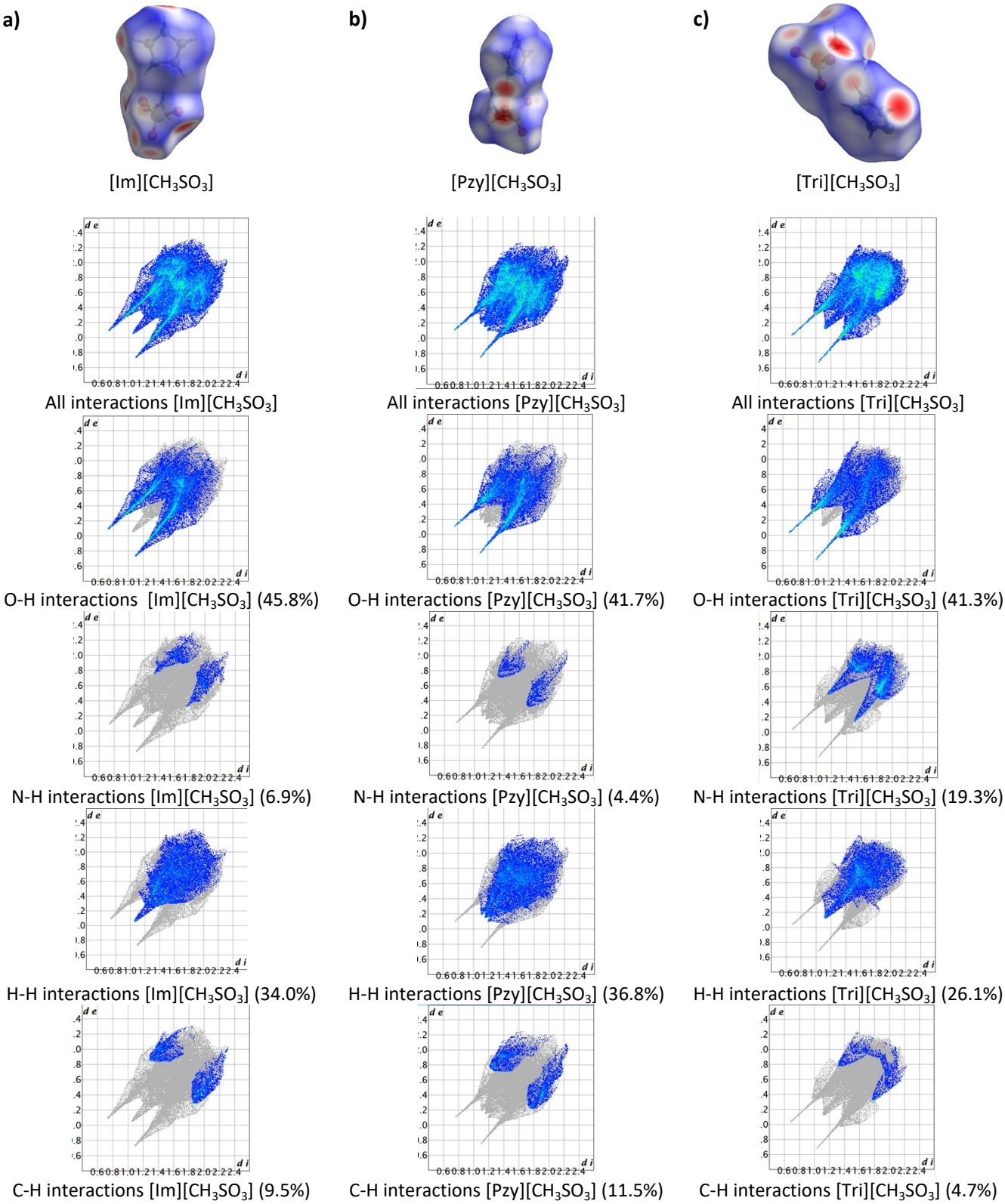

Figure S 55 Hirshfeld surface analysis of [Im][CH_3SO_3], [Pzy][CH_3SO_3], and [Tri][CH_3SO_3].

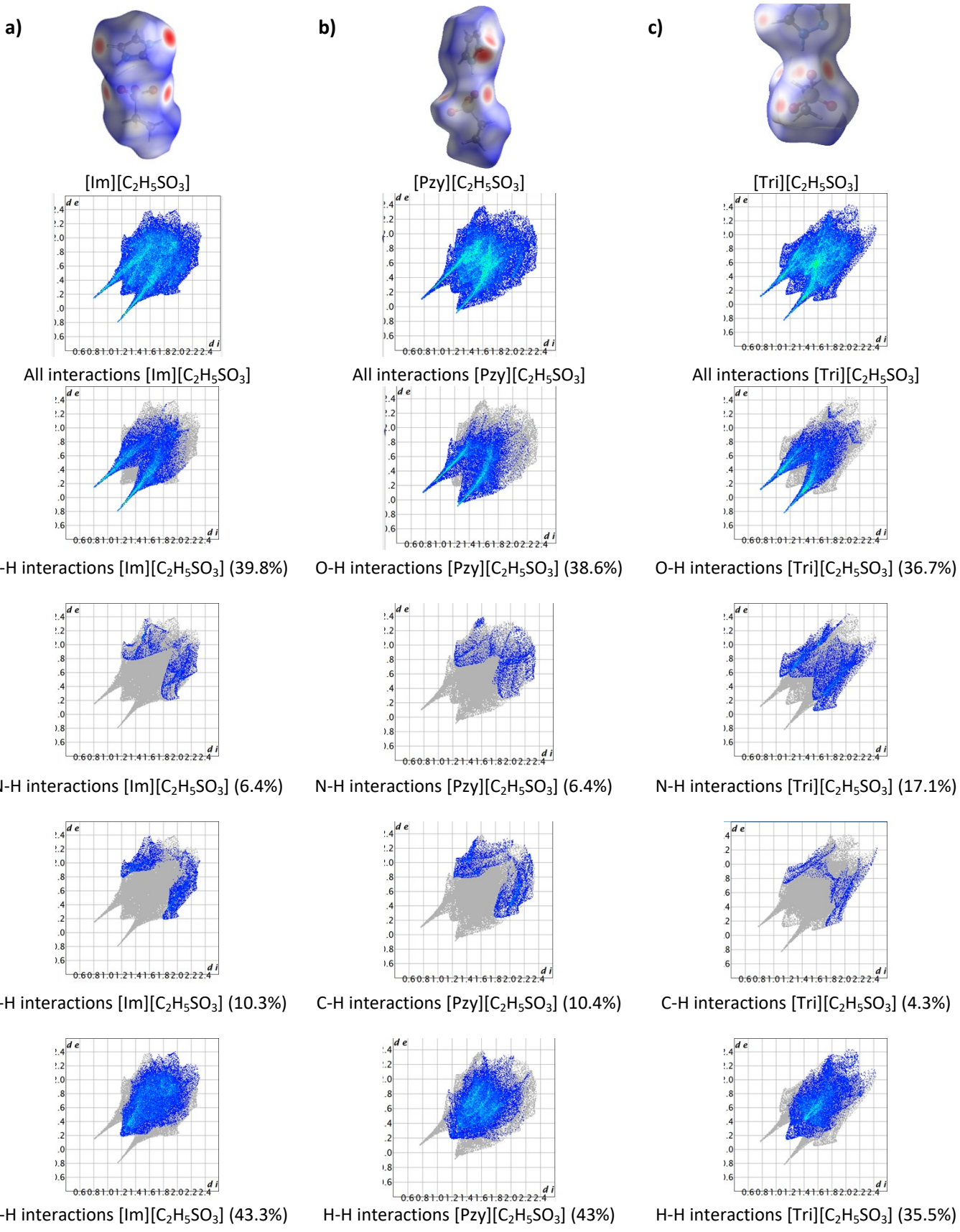

Figure S 56 Hirshfeld surface analysis of [Im][$C_2H_5SO_3$], [Pzy][$C_2H_5SO_3$], and [Tri][$C_2H_5SO_3$].

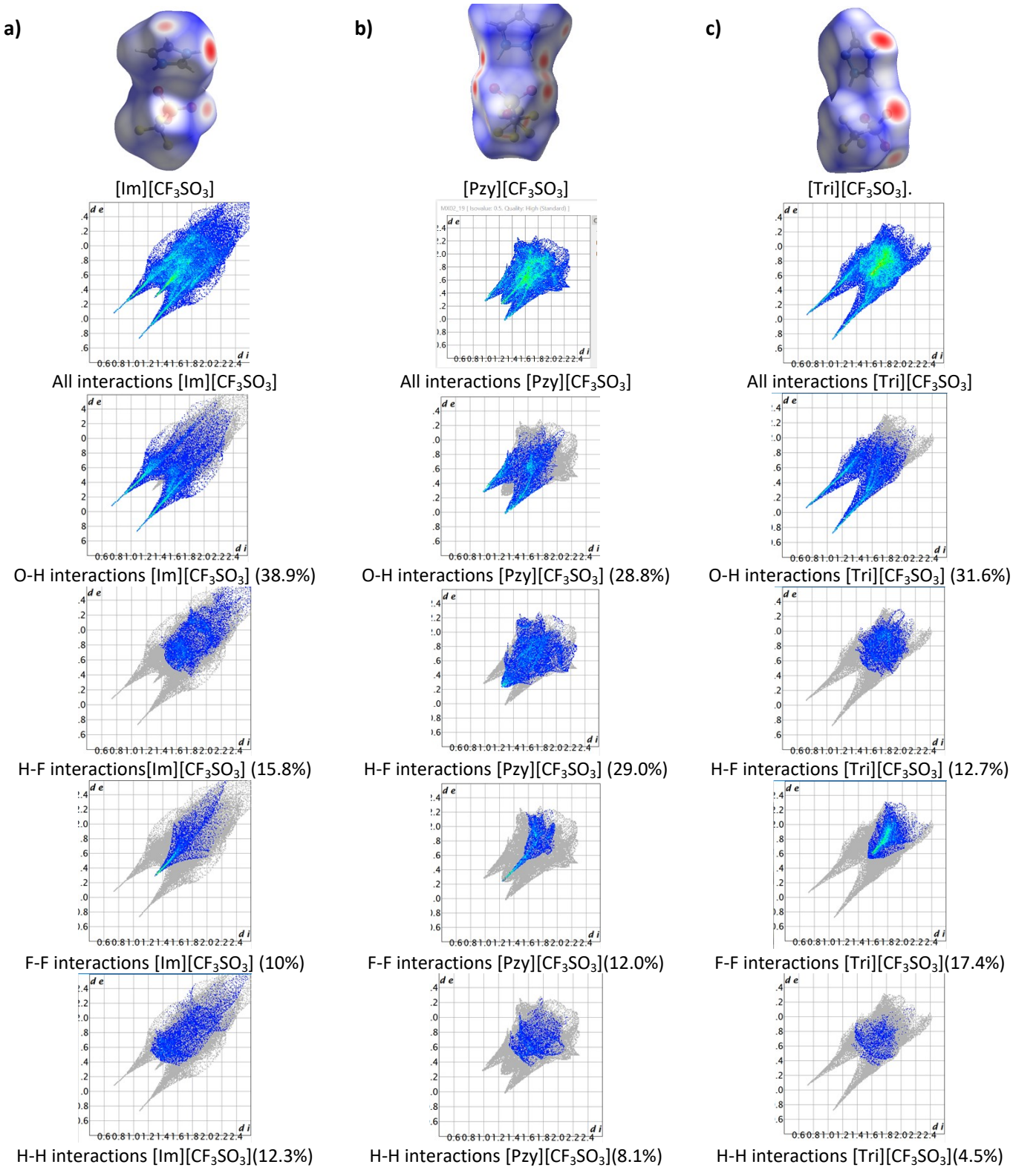

Figure S 57 Hirshfeld surface analysis of [Im][CF_3SO_3], [Pzy][CF_3SO_3], and [Tri][CF_3SO_3].

a)

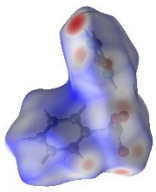

[Im][$C_6H_5SO_3$]

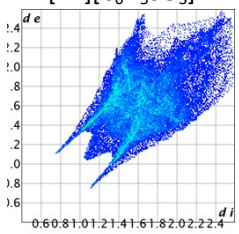

All interactions [Im][$C_6H_5SO_3$]

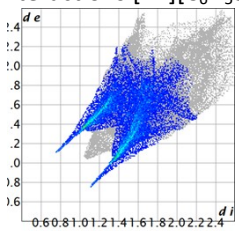

O-H interactions [Im][$C_6H_5SO_3$] (31%)

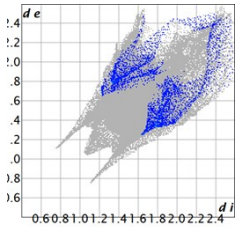

N-H interactions [Im][$C_6H_5SO_3$] (4.4%)

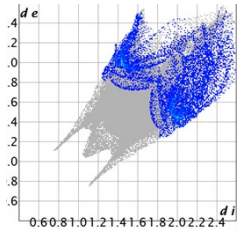

C-H interactions [Im][$C_6H_5SO_3$] (14.4%)

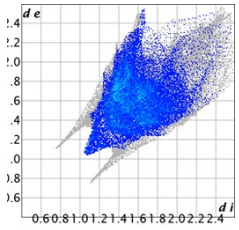

H-H interactions [Im][$C_6H_5SO_3$] (40.2%)

b)

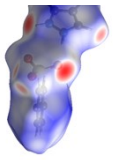

[Pzy][$C_6H_5SO_3$]

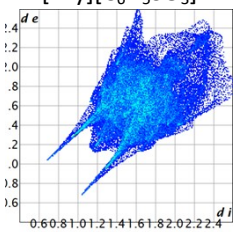

All interactions [Pzy][$C_6H_5SO_3$]

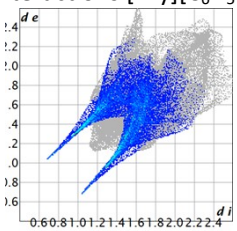

O-H interactions [Pzy][$C_6H_5SO_3$] (28.8%)

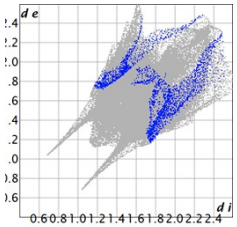

N-H interactions [Pzy][$C_6H_5SO_3$] (3.7%)

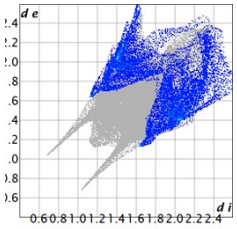

C-H interactions [Pzy][$C_6H_5SO_3$] (19.3%)

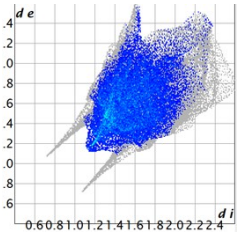

H-H interactions [Pzy][$C_6H_5SO_3$] (39.1)

c)

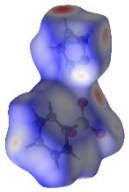

[Tri][$C_6H_5SO_3$]

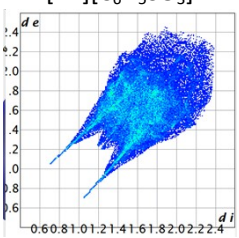

All interactions [Tri][$C_6H_5SO_3$]

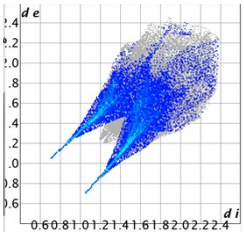

O-H interactions [Tri][$C_6H_5SO_3$] (32.1%)

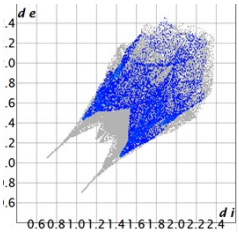

N-H interactions [Tri][$C_6H_5SO_3$] (12.7%)

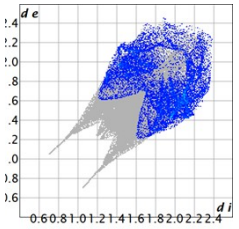

C-H interactions [Tri][$C_6H_5SO_3$] (16.1%)

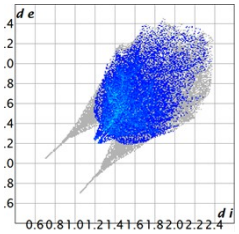

H-H interactions [Tri][$C_6H_5SO_3$] (29.5%)

Figure S 58 Hirshfeld surface analysis of [Im][$C_6H_5SO_3$], [Pzy][$C_6H_5SO_3$], and [Tri][$C_6H_5SO_3$].

6 Differential Scanning Calorimetry (DSC) plots

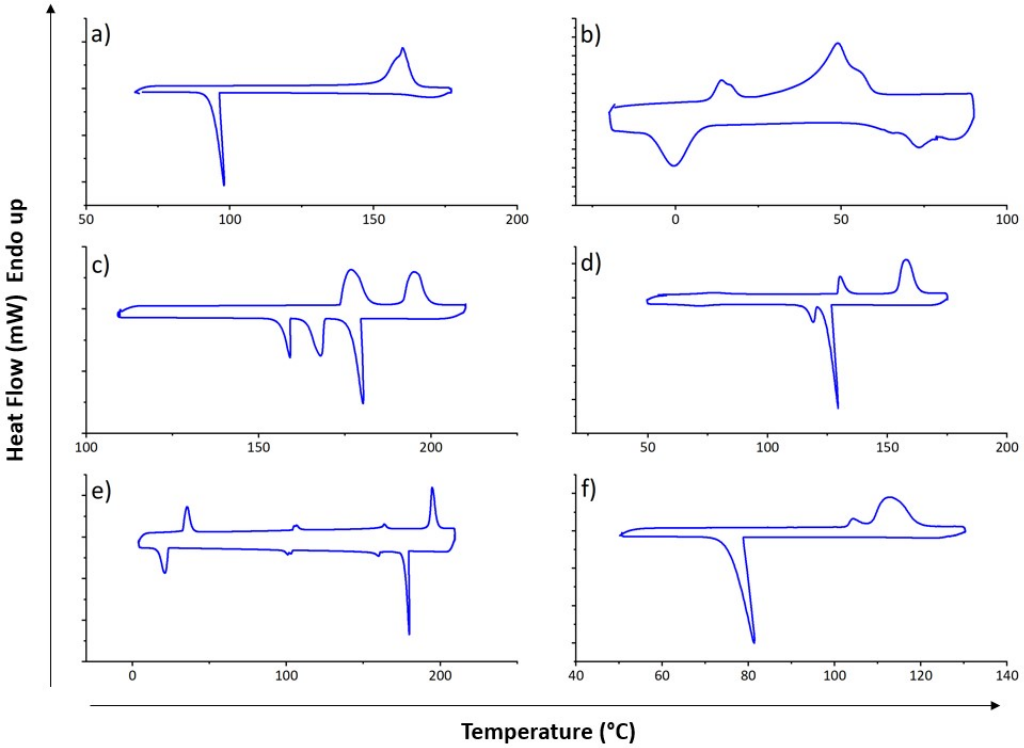

Figure S 59 Differential scanning calorimetry (DSC) traces of second heating/cooling cycle of a) [Im]Cl, b)[Im][HSO_4], c)[Im][CH_3SO_3], d)[Im][$C_2H_5SO_3$], e)[Im][CF_3SO_3] and [Im][$C_6H_5SO_3$].

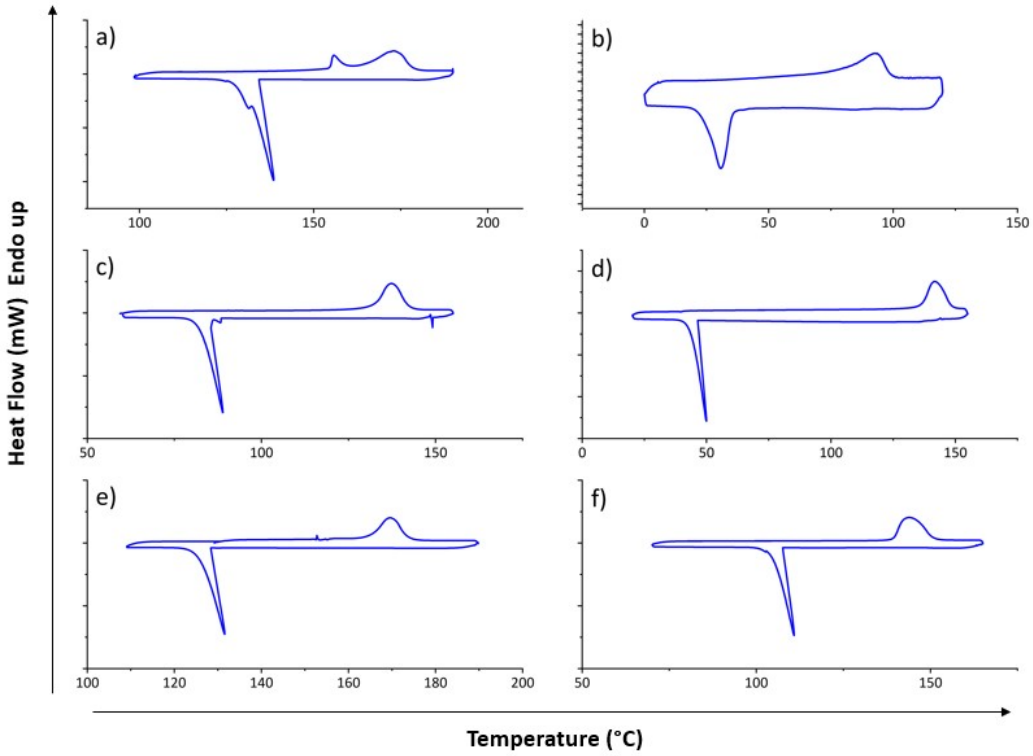

Figure S 60 Differential scanning calorimetry (DSC) traces of second heating/cooling cycle of a) [Tri]Cl, b)[Tri][HSO_4], c)[Tri][CH_3SO_3], d)[Tri][$C_2H_5SO_3$], e)[Tri][CF_3SO_3] and [Tri][$C_6H_5SO_3$].

7 Thermogravimetric analysis

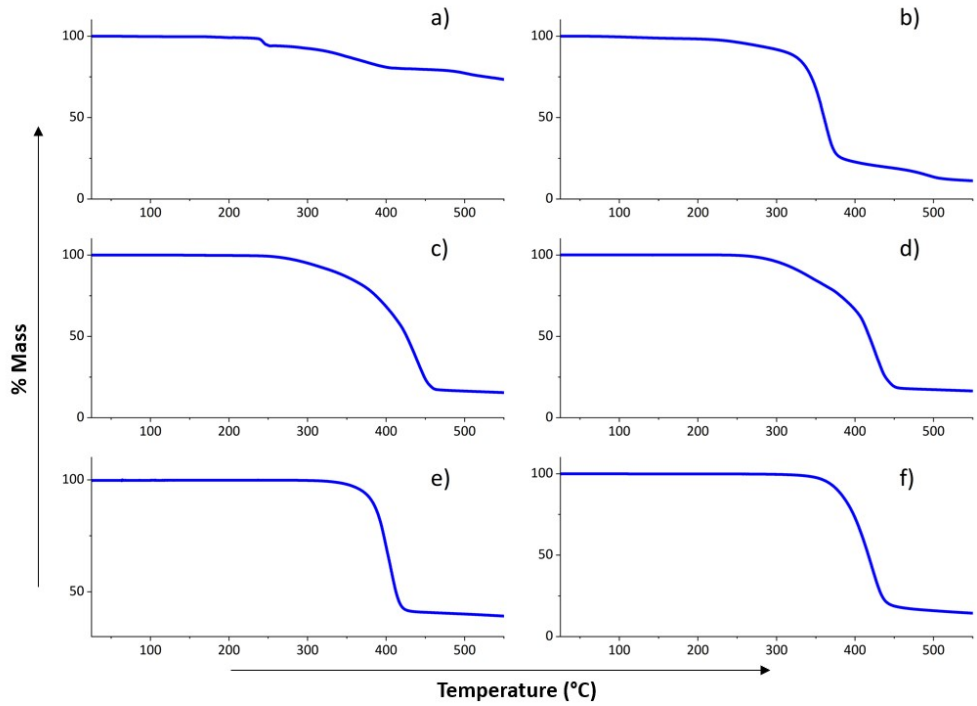

Figure S 61 Thermogravimetric analysis (TGA) plots of a)[Im]Cl, b) [Im][HSO_4], c) [Im][CH_3SO_3], d) [Im][$C_2H_5SO_3$], e)[Im][CF_3SO_3] and f)[Im][$C_6H_5SO_3$].

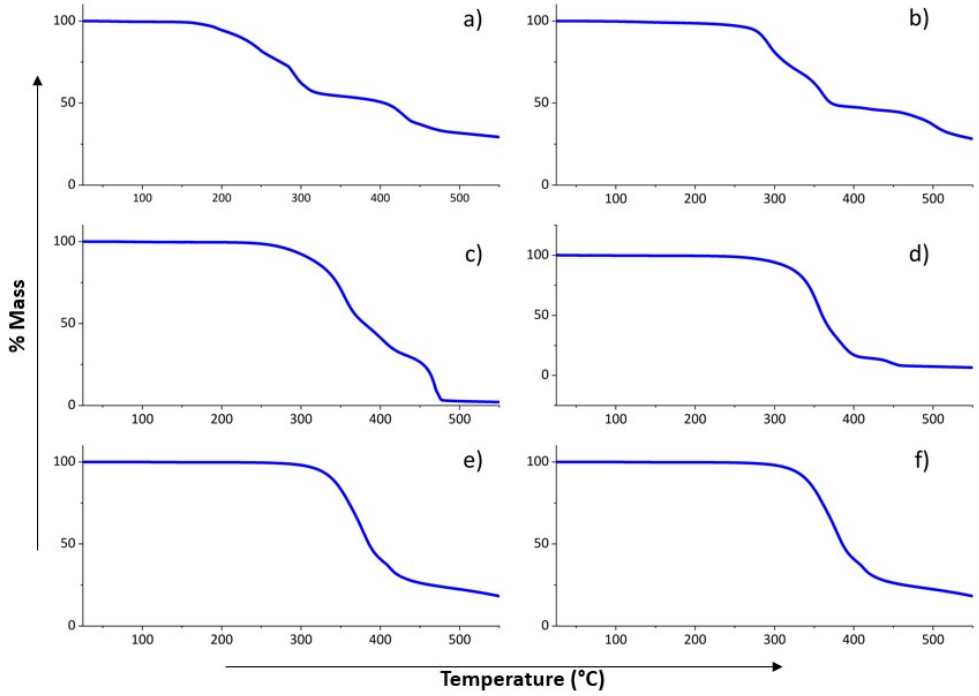

Figure S 62 Thermogravimetric analysis (TGA) plots of a)[Tri]Cl, b) [Tri][HSO_4], c) [Tri][CH_3SO_3], d) [Tri][$C_2H_5SO_3$], e)[Tri][CF_3SO_3] and f)[Tri][$C_6H_5SO_3$].

References

1. C. P. Brock and L. L. Duncan, *Chemistry of materials*, 1994, **6**, 1307-1312.
2. G. R. Desiraju, *CrystEngComm*, 2007, **9**, 91-92.
3. L. Xu, X. Mu, X.-G. Chen, H.-Y. Zhang and R.-G. Xiong, *Chemistry of Materials*, 2021, **33**, 5769-5779.
4. K. Matuszek, R. Vijayaraghavan, C. M. Forsyth, S. Mahadevan, M. Kar and D. R. MacFarlane, *ChemSusChem*, 2020, **13**, 159-164.
5. C. J. Adams, M. A. Kurawa and A. G. Orpen, *Dalton Transactions*, 2010, **39**, 6974-6984.
6. M. Bujak and J. Zaleski, *Zeitschrift für Naturforschung B*, 2002, **57**, 157-164.
7. J. Luo, J. Hu, W. Saak, R. Beckhaus, G. Wittstock, I. F. Vankelecom, C. Agert and O. Conrad, *Journal of Materials Chemistry*, 2011, **21**, 10426-10436.